Rho, J.M., Kim, D.W., Robbins, C.A., Anderson, G.D., and Schwartzkroin, P.A. (1999). Age-dependent differences in flurothyl seizure sensitivity in mice treated with a ketogenic diet. Epilepsy Res. *37*, 233–240.

Schwer, B., Bunkenborg, J., Verdin, R.O., Andersen, J.S., and Verdin, E. (2006). Reversible lysine acetylation controls the activity of the mitochondrial enzyme acetyl-CoA synthetase 2. Proc. Natl. Acad. Sci. USA *103*, 10224–10229.

Schwer, B., and Verdin, E. (2008). Conserved metabolic regulatory functions of sirtuins. Cell Metab. *7*, 104–112.

Scott, M.D., Baudendistel, L.J., and Dahms, T.E. (1992). Rapid separation of creatine, phosphocreatine and adenosine metabolites by ion-pair reversed-phase high-performance liquid chromatography in plasma and cardiac tissue. J. Chromatogr. *576*, 149–154.

Seufert, C.D., Graf, M., Janson, G., Kuhn, A., and Soling, H.D. (1974). Formation of free acetate by isolated perfused livers from normal, starved and diabetic rats. Biochem. Biophys. Res. Commun. *57*, 901–909.

Spiegelman, B.M., and Flier, J.S. (2001). Obesity and the regulation of energy balance. Cell *104*, 531–543.

Takamura, Y., Kitayama, Y., Arakawa, A., Yamanaka, S., Tosaki, M., and Ogawa, Y. (1985). Malonyl-CoA: Acetyl-CoA cycling. A new micromethod for determination of acyl-CoAs with malonate decarboxylase. Biochim. Biophys. Acta *834*, 1–7.

Takayasu, S., Sakurai, T., Iwasaki, S., Teranishi, H., Yamanaka, A., Williams, S.C., Iguchi, H., Kawasawa, Y.I., Ikeda, Y., Sakakibara, I., et al. (2006). A neuropeptide ligand of the G protein-coupled receptor GPR103 regulates feeding, behavioral arousal, and blood pressure in mice. Proc. Natl. Acad. Sci. USA *103*, 7438–7443.

Tanaka, T., Yamamoto, J., Iwasaki, S., Asaba, H., Hamura, H., Ikeda, Y., Watanabe, M., Magoori, K., Ioka, R.X., Tachibana, K., et al. (2003). Activation of peroxisome proliferator-activated receptor delta induces fatty acid beta-oxidation in skeletal muscle and attenuates metabolic syndrome. Proc. Natl. Acad. Sci. USA *100*, 15924–15929.

Teshigawara, K., Ogawa, W., Mori, T., Matsuki, Y., Watanabe, E., Hiramatsu, R., Inoue, H., Miyake, K., Sakaue, H., and Kasuga, M. (2005). Role of Kruppel-like factor 15 in PEPCK gene expression in the liver. Biochem. Biophys. Res. Commun. *327*, 920–926.

Wolfgang, M.J., Kurama, T., Dai, Y., Suwa, A., Asaumi, M., Matsumoto, S., Cha, S.H., Shimokawa, T., and Lane, M.D. (2006). The brain-specific carnitine palmitoyltransferase-1c regulates energy homeostasis. Proc. Natl. Acad. Sci. USA *103*, 7282–7287.

Yamamoto, J., Ikeda, Y., Iguchi, H., Fujino, T., Tanaka, T., Asaba, H., Iwasaki, S., Ioka, R.X., Kaneko, I.W., Magoori, K., et al. (2004). A Kruppel-like factor KLF15 contributes fasting-induced transcriptional activation of mitochondrial acetyl-CoA synthetase gene AceCS2. J. Biol. Chem. *279*, 16954–16962.

Yamashita, H., Kaneyuki, T., and Tagawa, K. (2001). Production of acetate in the liver and its utilization in peripheral tissues. Biochim. Biophys. Acta *1532*, 79–87.

Yang, H., Yang, T., Baur, J.A., Perez, E., Matsui, T., Carmona, J.J., Lamming, D.W., Souza-Pinto, N.C., Bohr, V.A., Rosenzweig, A., et al. (2007). Nutrient-sensitive mitochondrial NAD+ levels dictate cell survival. Cell *130*, 1095–1107.

THE JOURNAL OF BIOLOGICAL CHEMISTRY VOL. 284, NO. 11, pp. 7255–7263, March 13, 2009

Novel Mitochondrial Complex II Isolated from *Trypanosoma cruzi* Is Composed of 12 Peptides Including a Heterodimeric Ip Subunit*[S]

Received for publication, August 26, 2008, and in revised form, January 2, 2009 Published, JBC Papers in Press, January 2, 2009, DOI 10.1074/jbc.M806623200

Jorge Morales[‡1], Tatsushi Mogi[‡2], Shigeru Mineki[§], Eizo Takashima[‡3], Reiko Mineki[¶], Hiroko Hirawake[‡], Kimitoshi Sakamoto[‡], Satoshi Ōmura[‖], and Kiyoshi Kita[‡4]

From the [‡]Department of Biomedical Chemistry, Graduate School of Medicine, the University of Tokyo, Hongo, Bunkyo-ku, Tokyo 113-0033, the [§]Department of Applied Biological Science, Faculty of Science and Technology, Tokyo University of Science, Noda, Chiba 278-8510, the [¶]Division of Proteomics and BioMolecular Science, Juntendo University Graduate School of Medicine, Hongo, Bunkyo-ku, Tokyo 113-8421, and the [‖]Kitasato Institute for Life Sciences and Graduate School of Infection Control Sciences, Kitasato University, Minato-ku, Tokyo 108-8641, Japan

Mitochondrial respiratory enzymes play a central role in energy production in aerobic organisms. They differentiated from the α-proteobacteria-derived ancestors by adding non-catalytic subunits. An exception is Complex II (succinate: ubiquinone reductase), which is composed of four α-proteobacteria-derived catalytic subunits (SDH1–SDH4). Complex II often plays a pivotal role in adaptation of parasites in host organisms and would be a potential target for new drugs. We purified Complex II from the parasitic protist *Trypanosoma cruzi* and obtained the unexpected result that it consists of six hydrophilic (SDH1, $SDH2_N$, $SDH2_C$, and SDH5–SDH7) and six hydrophobic (SDH3, SDH4, and SDH8–SDH11) nucleus-encoded subunits. Orthologous genes for each subunit were identified in *Trypanosoma brucei* and *Leishmania major*. Notably, the iron-sulfur subunit was heterodimeric; $SDH2_N$ and $SDH2_C$ contain the plant-type ferredoxin domain in the N-terminal half and the bacterial ferredoxin domain in the C-terminal half, respectively. Catalytic subunits (SDH1, $SDH2_N$ plus $SDH2_C$, SDH3, and SDH4) contain all key residues for binding of dicarboxylates and quinones, but the enzyme showed the lower affinity for both substrates and inhibitors than mammalian enzymes. In addition, the enzyme binds protoheme IX, but SDH3 lacks a ligand histidine. These unusual features are unique in the Trypanosomatida and make their Complex II a target for new chemotherapeutic agents.

The parasitic protist *Trypanosoma cruzi* is the etiological agent of Chagas disease, a public health threat in Central and South America. These parasites are normally transmitted by reduviid bugs via the vector feces after a bug bite and also via transfusion of infected blood. About 16–18 million people are infected, and 100 million are at risk, but there are no definitive chemotherapeutic treatments available (1). Despite having potential pathways for oxidative phosphorylation (2), all trypanosomatids (*Trypanosoma* and *Leishmania* species) analyzed so far are characterized by incomplete oxidation of glucose with secretion of end products, such as succinate, alanine, ethanol, acetate, pyruvate, and glycerol (3, 4) (Fig. 1). Major routes for formation of succinate in *Trypanosoma brucei* are via NADH-dependent fumarate reductase in glycosomes and mitochondria (5, 6). In trypanosomatid mitochondria, the Krebs cycle is inefficient, and pyruvate is principally converted to acetate via acetate:succinate CoA transferase (7). A part of the Krebs cycle operates the utilization of histidine in the insect stage of *T. cruzi* (8).

Mitochondrial Complex II (succinate:quinone reductase (SQR)[5] and succinate dehydrogenase (SDH)) serves as a membrane-bound Krebs cycle enzyme and often plays a pivotal role in adaptation of parasites to environments in their host (9, 10). In general, Complex II consists of four subunits (11). A flavoprotein subunit (SDH1, Fp) and an iron-sulfur subunit (SDH2, Ip) form a soluble heterodimer, which then binds to a membrane anchor heterodimer, SDH3 (CybL) and SDH4 (CybS). SDH1 contains a covalently bound FAD and catalyzes the oxidation of succinate to fumarate. SDH2 transfers electrons to ubiquinone via the [2Fe-2S] cluster in the N-terminal plant-type ferredoxin domain (Ip_N) and the [4Fe-4S] and [3Fe-4S] clusters in the C-terminal bacterial ferredoxin domain (Ip_C). Ubiquinone is bound and reduced in a pocket provided by SDH2, SDH3, and SDH4 (12–14). SDH3 and SDH4 contain three transmembrane helices and coordinate protoheme IX via histidine in the second helices of each subunit (11–14).

* This work was supported in part by Grant-in-aid for Scientific Research 20570124 (to T. M.), Creative Scientific Research Grant 18GS0314 (to K. K.), Grant-in-aid for Scientific Research on Priority Areas 18073004 (to K. K.) from the Japanese Society for the Promotion of Science, and Targeted Proteins Research Program (to K. K.) from the Japanese Ministry of Education, Science, Culture, Sports and Technology (MEXT). The costs of publication of this article were defrayed in part by the payment of page charges. This article must therefore be hereby marked "*advertisement*" in accordance with 18 U.S.C. Section 1734 solely to indicate this fact.

[S] The on-line version of this article (available at http://www.jbc.org) contains supplemental Table S1.

[1] Supported by a Japanese Government scholarship from Ministry of Education, Science, Culture, Sports and Technology.

[2] To whom correspondence may be addressed. Tel.: 81-3-5841-3526; Fax: 81-3-5841-3444; E-mail: tmogi@m.u-tokyo.ac.jp.

[3] Present address: Dept. of Microbiology, School of Life Dentistry at Tokyo, Nippon Dental University, Tokyo 102-8159, Japan.

[4] To whom correspondence may be addressed. Tel.: 81-3-5841-3526; Fax: 81-3-5841-3444; E-mail: kitak@m.u-tokyo.ac.jp.

[5] The abbreviations used are: SQR, succinate:quinone reductase; hrCNE, high resolution clear native electrophoresis; IC_{50}, the 50% inhibitory concentration; Ip_N, the N-terminal plant-type ferredoxin domain; Ip_C, the C-terminal bacterial ferredoxin domain; DCIP, 2,4-dichlorophenolindophenol; SML, sucrose monolaurate; Tricine, *N*-[2-hydroxy-1,1-bis(hydroxymethyl)ethyl]-glycine; MOPS, 3-(*N*-morpholino)propanesulfonic acid; Q_n, ubiquinone-*n*.

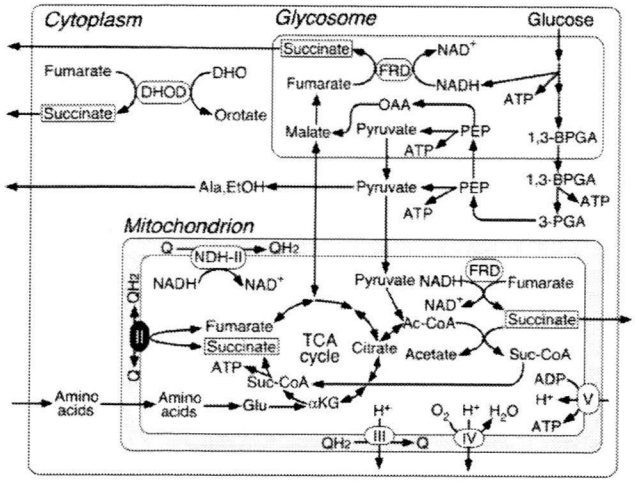

FIGURE 1. **Metabolic pathways in *T. cruzi*.** Incomplete oxidation of glucose takes place in glycosomes and mitochondria, and end products such as succinate, L-alanine, ethanol, and acetate are excreted from parasites (3, 4). Cytoplasmic dihydroorotate (*DHO*):fumarate reductase (*DHOD*) contributes succinate production (6).

Parasitic nematodes adapted to hypoxic host environments often have modified respiratory chains. Many adult parasites perform fumarate respiration by expressing a stage-specific isoform of Complex II (9, 10). *Hemonchus contortus* uses an isoform for SDH2 (9), whereas *Ascaris suum* uses isoforms for SDH1 and SDH4 (10). To explore the adaptive strategy in a parasitic protist, we isolated mitochondria from axenic culture of *T. cruzi* epimastigotes and characterized the purified Complex II. Our results demonstrated for the first time that *T. cruzi* Complex II is an unusual supramolecular complex with a heterodimeric iron-sulfur subunit and seven novel noncatalytic subunits. Purified enzyme showed reduced binding affinities for both substrates and inhibitors. Because this novel structural organization is conserved in all trypanosomatids (2, 15, 16), parasite Complex II would be a potential target for the development of new chemotherapeutic agents for trypanosomiasis and leishmaniasis.

EXPERIMENTAL PROCEDURES

Preparation of Mitochondria—*T. cruzi* strain Tulahuhen was grown statically for 6–7 days at 26 °C in 300-cm^2 cell culture flasks (Falcon, BD Biosciences) containing 250 ml of the modified LIT medium (17), supplemented with 0.1% (w/v) glucose, 0.001% (w/v) hemin (Sigma), and 5% (v/v) fetal bovine serum (MP Biochemicals). Mitochondria were isolated from epimastigotes by the differential centrifugation method (18) with slight modifications. Parasites grown to $6-8 \times 10^7$ cells/ml were washed with buffer A (20 mM Tris-HCl, pH 7.2, 10 mM NaH_2PO_4, 1 mM sodium EDTA, 1 mM dithiothreitol, 0.225 M sucrose, 20 mM KCl, and 5 mM $MgCl_2$). Cells were disrupted by grinding with silicon carbide (Carborundum 440 mesh; Nacalai Tesque, Kyoto, Japan) in the presence of a minimum volume of buffer B (25 mM Tris-HCl, pH 7.6, 1 mM dithiothreitol, 1 mM sodium EDTA, 0.25 M sucrose, and EDTA-free Complete protease inhibitor mixture (Roche Applied Science)). The resultant cell paste was resuspended in buffer B and centrifuged at 500 × *g* for 5 min and 1000 × *g* for 15 min to remove silicon carbide and nuclear fraction, respectively. The mitochondrial fraction was recovered upon centrifugation of the last supernatant at 10,000 × *g* for 15 min, washed three times in buffer B, and resuspended to a protein concentration of ~30 mg/ml and kept at −80 °C until use.

TABLE 1
Purification of complex II from *T. cruzi* mitochondria

Step	Protein	Succinate:DCIP reductase		Yield	Purification
	mg	*units*	*units/mg*	*%*	*-fold*
Mitochondria	314	27	0.085	100	1.0
SML extract	141	22	0.16	83	1.9
Source 15Q	7.8	7.6	0.97	28	12
Superdex 200 (1st)	1.3	1.4	1.09	5.3	13
Superdex 200 (2nd)	0.15	0.43	2.87	1.6	34

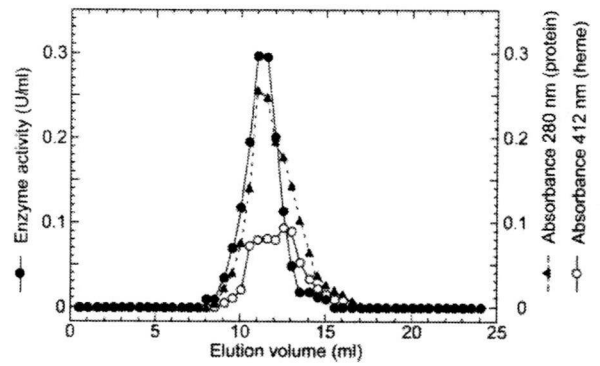

FIGURE 2. **Elution profile of *T. cruzi* Complex II on Superdex 200 chromatography.** Complex II fractions from the first gel filtration chromatography with a Superdex 200-pg column were concentrated and rechromatographed at the flow rate of 0.25 ml/min. Aliquots were collected every 0.5 ml. Elution profiles for proteins and cytochromes were monitored at 280 (▲) and 412 nm (○), respectively, and the enzyme activity (●) was measured as decylquinone-mediated succinate:DCIP reductase.

Isolation of Complex II—All steps were carried out at 4 °C. Mitochondrial fraction (~300 mg of protein from 10 liters culture) was brought to 70 ml with buffer C (10 mM KP_i, pH 7.5), 1 mM sodium EDTA, 1 mM sodium malonate, EDTA-free Complete protease inhibitor mixture (Roche Applied Science) (2 tablets/50 ml), 1% (w/v) sucrose monolaurate SM-1200 (SML) (Mitsubishi-Kagaku Foods Co., Tokyo, Japan)). The mixture was stirred for 30 min and centrifuged at 200,000 × *g* for 1 h. The supernatant was loaded at 1 ml/min onto a Source 15 Q column (1.6 inner diameter × 10 cm; GE Healthcare), equilibrated with buffer C containing 0.1% SML. After washing with 5 volumes of the same buffer, proteins were eluted with a 200-ml linear gradient of NaCl from 0 to 150 mM at 2 ml/min. Active fractions were concentrated to ~250 μl by ultrafiltration with Amicon Ultra-4 (molecular weight cutoff 100,000, Millipore) and subjected to gel filtration FPLC with a Superdex 200-pg 10/300 GL column (1 cm inner diameter × 30 cm; GE Healthcare) at 0.25 ml/min in 20 mM MOPS-NaOH, pH 7.2, containing 1 mM sodium EDTA, 1 mM sodium malonate, 150 mM NaCl, and 0.1% SML. Peak fractions were rechromatographed as above, and purified enzyme was concentrated and stored at −80 °C until use.

Identification of Complex II Subunits—The purified enzyme was subjected to 12.5% SDS-PAGE, and subunits were transferred to an Immobilon-P membrane (Millipore), followed by

staining with Coomassie Brilliant Blue R-250 (19, 20). Five or ten N-terminal amino acid residues were determined with a Procise 494 HT (Applied Biosystems) or an Hp G1005A (Hewlett-Packard Co.) Protein Sequencing System at the Bio-Medical Research Center of Juntendo University or APRO Life Science Institute, Inc. (Tokushima, Japan). When the N terminus was blocked, protein bands were digested with trypsin, and internal peptide sequences were determined (20). Genes coded for Complex II subunits were identified with BLASTP in the *T. cruzi* genome data base (15).

Phase Partitioning of Mitochondrial Fraction with Triton X-114—Phase partitioning by Triton X-114 was performed as described previously (21) with a slight modification. A total of 2–3 mg of mitochondrial fraction was resuspended in 1 ml of Tris-HCl, pH 7.5, 150 mM NaCl, 1 mM EDTA, 2 mM sodium malonate, Complete protease inhibitors mixture (Roche Applied Science) (2 tablets/50 ml), protease inhibitors mixture for mammalian cell and tissue extracts (Sigma) (10 μl/ml), and 2% (v/v) Triton X-114. The mixture was incubated for 30 min on ice and kept at −30 °C overnight. After thawing, the insoluble material was removed by centrifugation at 4 °C, and the supernatant was incubated for 10 min at 37 °C and centrifuged at 2000 × *g* for 10 min to separate the aqueous and detergent-rich phases. The aqueous phase was brought to 2% (v/v) Triton X-114, whereas the detergent-rich fraction was brought to 1 ml with the above buffer. After incubation on ice for 10 min, samples were incubated at 37 °C for 10 min and phases separated as before. This wash step was repeated three times. Finally, the samples were dialyzed and concentrated by Amicon Ultra-4 (Millipore) in the presence of 50 mM imidazole, 50 mM NaCl, 6 mM aminocaproic acid, 0.05% (w/v) deoxycholate, and 0.1% (w/v) SML, pH 7, and kept at −80 °C until use.

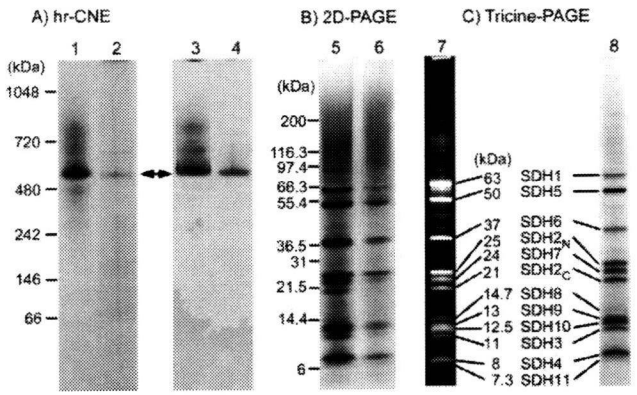

FIGURE 3. **Electrophoresis analysis of *T. cruzi* Complex II.** *A*, purified Complex II (2 μg; *lanes 1* and *3*) and the detergent-rich fraction from the phase partitioning by Triton X-114 of the mitochondrial fraction (60 μg; *lines 2* and *4*) were subjected to hrCNE. Proteins were stained by Coomassie Brilliant Blue (*left panel*), and Complex II was visualized by SDH activity staining (*right panel*). *B*, proteins of Complex II showing SDH activity in *A* were analyzed by 10–20% Tricine SDS-PAGE and visualized by silver stain (*lane 5*, pure complex; *lane 6*, detergent-rich fraction). *C* shows the subunit composition of the pure Complex II from *T. cruzi* stained by SYPRO ruby (*lane 7*) or silver stain (*lane 8*). Molecular weight standards used are NativeMark (Invitrogen, *lane 1*) and Mark 12 unstained standards (Invitrogen, *lanes 5* and *7*).

Enzyme Assay—Decylubiquinone-mediated succinate-2,4 dichlorophenolindophenol (DCIP) reductase activity was measured at 25 °C in 100 mM potassium phosphate, pH 7.4, containing 1 mM $MgCl_2$, 2 mM KCN, 0.1 mM antimycin A (Sigma), and 0.1% SML with 63 μM decylubiquinone (Sigma) *plus* 60 μM DCIP. After 2 min of incubation, reduction of DCIP (ϵ_{600} = 21 mM^{-1} cm^{-1}) was measured in the presence of 10 mM succinate. SQR activity was determined with 40 μM ubiquinone-2 (Q_2) (Sigma, ϵ_{278} = 12.3 mM^{-1} cm^{-1}). Kinetic analysis was done with KaleidaGraph version 4.0 (Synergy Software).

Miscellaneous—High resolution clear native electrophoresis (hrCNE) (22) was performed with 4–16% Novex gels (Invitrogen) using 0.02% dodecylmaltoside and 0.05% sodium deoxycholate for the cathode buffer additives, and the Complex II band was visualized by the activity staining (23) or Coomassie Brilliant Blue. Tricine-PAGE analysis was done with Novex 10–20% Tricine gels (Invitrogen), and proteins bands were sequentially stained by Sypro ruby (Invitrogen) and silver. During purification the succinate-decylubiquinone-DCIP reduc-

TABLE 2
Identification of genes encoding subunits for *T. cruzi* complex II

Subunit[a]	Sequence confirmed[b]	Accession number or RefSeq ID at NCBI (haplotype,[c] M_r)	Identity[d]	TM[e]
			%	
SDH1	Ser^{10}–Met^{19}	AB031741 (NE, 66,974), XP_809281 (E, 18,231)	59	0
SDH5	Ala^{10}–Leu^{19}	XP_818124 (NE, 53,831), XP_810172 (E, 20,788)	16	0
$SDH2_N$	Ser^{188}–Arg^{196}, Lys^{201}–Ile^{204}, Gly^{221}–Asn^{223}, Glu^{267}–Ile^{269}	XP_814994 (merged, 32,232)[f]	24 (37)	0
$SDH2_C$	Pro^{2}–Leu^{6}	XP_803796 (NE, 21,352), XP_806126 (E, 21,379)	25 (43)	0
SDH6a	Val^{19}–Val^{28}	XP_809065 (NA, 36,077), XP_812789 (NA, 36,035)	15	0
SDH6b	Val^{19}–Val^{28}	XP_813603 (NA, 36,133), XP_813645 (NA, 36,039)	14	0
SDH7	Ile^{26}–Leu^{35}	XP_813318 (NE, 28,218), XP_820239 (E, 28,202)	22	0
SDH3	Val^{2}–Phe^{11}	XP_809410 (NE, 12,176), XP_810064 (E, 12,204)	29	1
SDH4	Phe^{39}–Thr^{48}	XP_808211 (E, 13,957), XP_816430 (NE, 13,975)	27	2
SDH8	Gly^{5}–Met^{16}	XP_809192 (NE, 16,199), XP_817545 (E, 16,143)	ND[g]	2
SDH9	Ile^{10}–Pro^{19}	XP_807105 (merged, 15,736)	ND	1
SDH10	Pro^{25}–Val^{33}	XP_808894 (NE, 15,565), XP_808903 (E, 15,554)	ND	1
SDH11	Phe^{20}–Cys^{29}	XP_814088 (E, 10,346), XP_814509 (NE, 10,337)	ND	1

[a] Alleles were named as SDH3-1 (XP_809410) and SDH3-2 (XP_810064) in the order of the accession numbers, except for SDH5.
[b] These are N-terminal sequences except for $SDH2_N$ and SDH8, where the N-terminal residues were blocked.
[c] Homozygous alleles located in a merged assembly of Esmeraldo (E) and non-Esmeraldo (NE) homologous sequences whose different copies were merged genes during the genome assembly are indicated by "merged." Haplotypes for gene with more than two copies in the genome that does not belong to a merged region are not assigned (NA).
[d] Identity % to counterparts in human were as follows: SDH1 (D30648), SDH2 (P21912), SDH3 (Q99643), or SDH4 (O14521). In parentheses, the identity % of $SDH2_N$ and $SDH2_C$ that correspond to either Met^{1}–Pro^{155} (Ip_N domain) or Tyr^{156}–Val^{280} (Ip_C domain), respectively, of human SDH2 is shown. Identity % for truncated forms of SDH1 and SDH5 (SDH1-2 and SDH5-2) in the Esmeraldo haplotype was 66 and 20%, respectively.
[e] Transmembrane segments (TM) were estimated with TMHMM (52) and SOSUI (53).
[f] SDH2N from other trypanosomatids lack Met^{1} to Arg^{42} of $TcSDH2_N$.
[g] ND indicates not determined because these hydrophobic sequences are a highly divergent form of mammalian sequences.

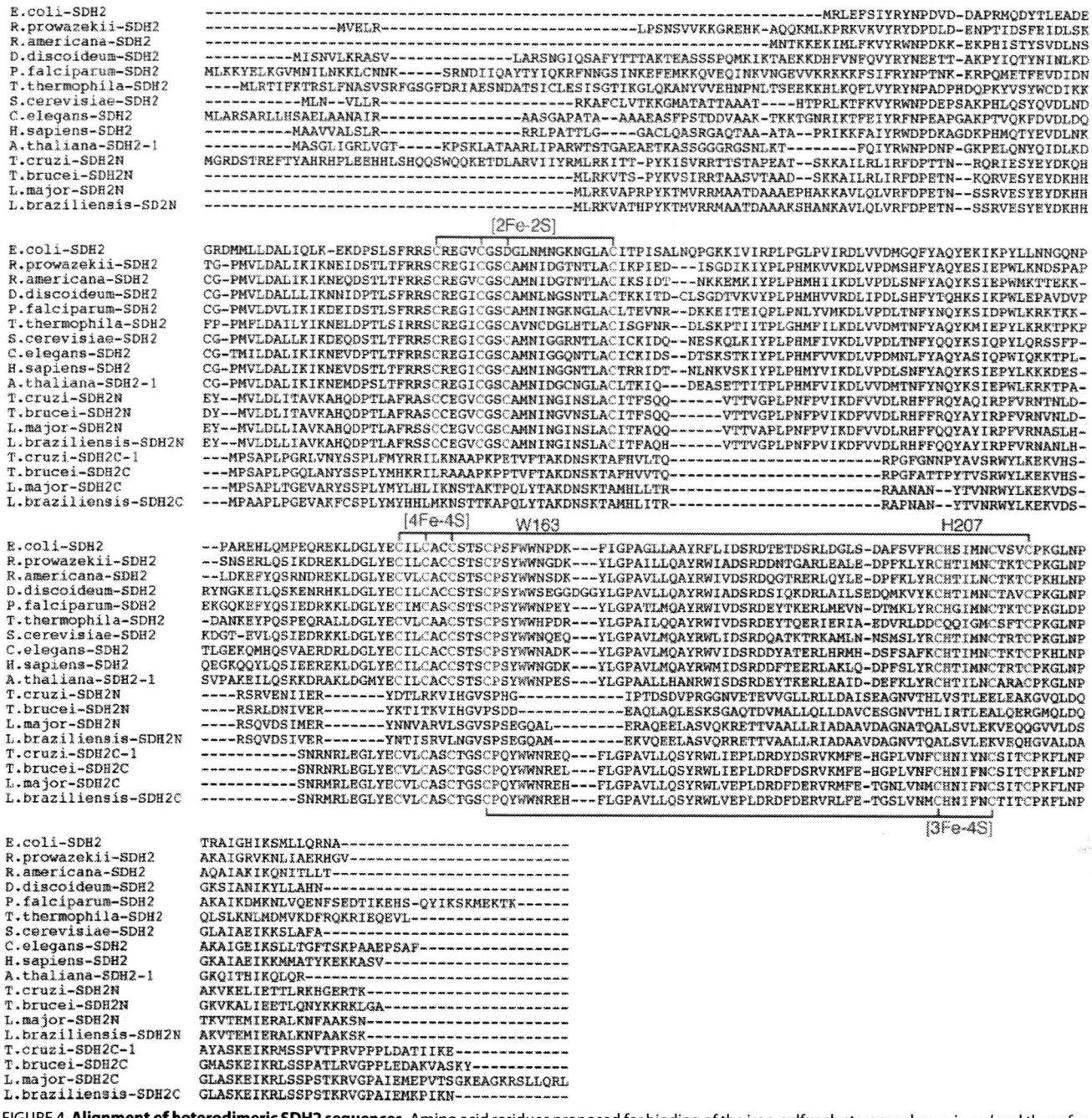

FIGURE 4. **Alignment of heterodimeric SDH2 sequences.** Amino acid residues proposed for binding of the iron-sulfur clusters are shown in *red* and those for the quinone binding in *blue*. Residue numbers refer to the *E. coli* SDH2 (SdhB) sequence. GenBank™ accession numbers for $SDH2_N$ and $SDH2_C$ sequences used are *T. cruzi* (XP_814994 and XP_803796), *T. brucei* (XP_847169 and XP_826981), and *L. major* (XP_001683488 and XP_001682013). Other SDH2 sequences used are *E. coli* (NP_415252), *Rickettsia prowazekii* (Q9ZEA1), *Reclinomonas americana* (NP_044798), *Dictyostelium discoideum* (XP_646559), *Plasmodium falciparum* (D86574), *Tetrahymena thermophila* (XP_001024894), *S. cerevisiae* (NP_012774), *Caenorhabditis elegans* (NP_495992), *H. sapiens* (NP_002991), and *A. thaliana* (NP_189374).

tase activity was monitored in a microplate spectrophotometer (Benchmark Plus, Bio-Rad). Kinetics and UV-visible absorption spectra were determined at room temperature with a V-660 UV-visible spectrophotometer (Jasco, Tokyo, Japan). Protoheme IX and protein concentrations were determined by pyridine hemochromogen method (24) and the micro BCA method (Pierce), respectively. Sequence alignment was done with ClustalX 2.0 (25).

RESULTS AND DISCUSSION

Isolation of T. cruzi Complex II—To determine the molecular organization of *T. cruzi* Complex II, we purified this enzyme from epimastigote mitochondria by ion-exchange and gel filtration chromatography using the nonionic detergent sucrose monolaurate (Table 1). Decylubiquinone-mediated succinate: DCIP reductase activity was eluted as a single peak at each step

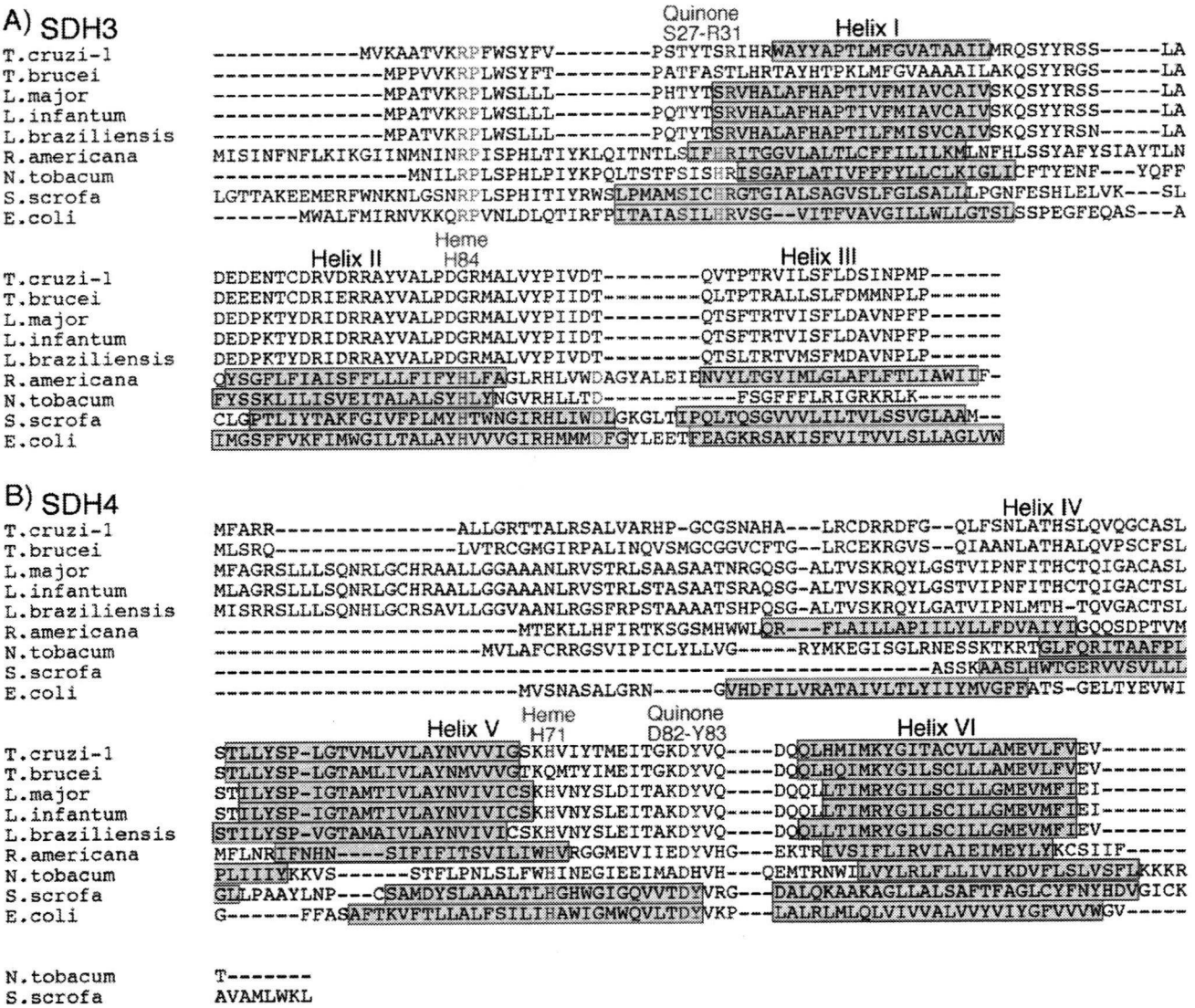

FIGURE 5. **Alignments of SDH3 (*A*) and SDH4 (*B*) sequences.** Amino acid residues proposed for binding of protoheme IX are shown in *red* and those for the quinone binding in *blue*. Other conserved residues are indicated by *green*. Transmembrane helices found in *E. coli* (Protein Data Bank code 1NEK) and porcine (Protein Data Bank code 1ZOY) Complex II are shown by *red rectangles*, and transmembrane helices predicted by TMHMM are indicated by *blue rectangles*. TMHMM failed to predict transmembrane helices in *T. brucei* SDH3. Residue numbers refer to *E. coli* SDH3 (SdhC) and SDH4 (SdhD). GenBank™ accession numbers for SDH3 and SDH4 sequences used are *T. cruzi* (XP_809410, XP_808211), *T. brucei* (XP_845531, XP_823384), *L. major* (XP_001684890, XP_001685874), *L. infantum* (XP_001467132), *L. brasiliensis* (XP_001566908, XP_001567905), *R. americana* (NP_044796, NP_044797), *Nicotiana tobacum* (YP_173376, YP_173457), *Sus scrofa* (1ZOY_C, 1ZOY_D), and *E. coli* (NP_415249, NP_415250).

and co-eluted with proteins and *b*-type cytochrome(s) at the second Superdex 200 chromatography (Fig. 2). Specific activity was increased 34-fold to 2.9 units/mg proteins, and the yield was ~2%. A hrCNE of the pure protein identified *T. cruzi* Complex II as an ~550-kDa complex (Fig. 3, *lanes 1* and *3*), which is 4-fold larger than bovine and yeast Complex II (130 kDa) and potato Complex II (150 kDa) (26, 27). Upon phase partitioning of the mitochondrial fraction with Triton X-114, the Complex II of *T. cruzi* was found only in the detergent-rich fraction (data not shown). Analysis of the detergent-rich fraction by hrCNE showed the Complex II as a single band at the same position as the pure enzyme (~550 kDa) (Fig. 3, *lanes 2* and *4*). These results indicated that the purified Complex II was obtained in its intact form. Interestingly, second dimensional analysis of both the purified Complex II and the detergent-rich fraction from phase partitioning with Triton X-114 with SDH activity showed that *T. cruzi* Complex II is composed of 12 subunits (Fig. 3, *lanes 5* and *6*). The same subunit composition was obtained by immunoaffinity purification of the partially purified enzyme (data not shown). The apparent molecular weight of the subunits ranges from 7.3 to 63 kDa (Fig. 3, *lanes 7* and *8*). Assuming the presence of equimolar amounts of subunits, a total molecular mass of Complex II would be 286.5 kDa, indicating that *T. cruzi* Complex II is a homodimer.

Identification of Genes Coded for Subunits—We determined N-terminal sequences (or internal peptide sequences in case of $SDH2_N$ and SDH8) of all subunits and identified genes coded for SDH1-1, $SDH2_N$, $SDH2_C$, SDH5–SDH7 (hydrophilic sub-

units), SDH3, SDH4, and SDH8–SDH11 (hydrophobic subunits) (Table 2). All subunits, except SDH1-1, are trypanosomatid-specific and structurally unrelated to plant-specific soluble subunits (AtSDH5–AtSDH8, 5–18 kDa) (27–29). All genes (except SDH6 with four copies) are present as two copies, which are assigned to either Esmeraldo or non-Esmeraldo haplotype (haploid genotype) in *T. cruzi* subgroup IIe. In contrast, only one copy each of the orthologues is present in *T. brucei*, *Leishmania major*, *Leishmania infantum*, and *Leishmania braziliensis* (supplemental Table S1). N-terminal sequence analysis of SDH3 and SDH7 showed that yields of two isoforms are similar (*i.e.* SDH3-1:SDH3-2 = 63:37, and SDH7-1:SDH7-2 = 54:46), indicating that isoforms are expressed from each haplotype. Because truncated isoforms for SDH1 and SDH5 in the Esmeraldo haplotype (see below) are not assembled into the 12-subunit complex and $SDH2_N$ and SDH9 isoforms have the identical sequence, 512 ($= 1^4 \times 4^1 \times 2^{(12-5)}$) kinds of heterogeneity may exist in the *T. cruzi* Complex II monomer (Table 2).

Flavoprotein Subunit—SDH1-1 (63-kDa band in Tricine-PAGE) cross-reacted with the antiserum against bovine SDH1 (data not shown) and is highly homologous to counterparts in *T. brucei* (93% identity), *L. major* (90%), *Homo sapiens* (59%), *Arabidopsis thaliana* (62%), *Saccharomyces cerevisiae* (61%), and *Escherichia coli* (48%, SdhA). Amino acid residues proposed for dicarboxylate binding and a FAD ligand histidine (12–14) are all conserved in SDH1-1. SDH1-1 and SDH5-1 of the non-Esmeraldo haplotype share a weak sequence similarity in the entire region, but the latter lacks amino acid residues responsible for FAD and dicarboxylate binding. In the Esmeraldo haplotype, SDH1-2 and SDH5-2 are truncated and contain only Met^1 to Gly^{167} of TcSDH1-1 and Ile^{305} to Met^{486} of TcSDH5-1, respectively (Table 2). These findings suggest that TcSDH1-1, TcSDH1-2, TcSDH5-1, and TcSDH5-2 might have evolved by gene duplication and subsequent degeneration.

Iron-Sulfur Subunit—Sequence analysis of the 25- and 21-kDa band proteins revealed that they contain the plant ferredoxin domain (Ip_N) and bacterial ferredoxin domain (Ip_C) of canonical SDH2 (Ip) in the N- and C-terminal half, respectively (Fig. 4). Sequence identities of Ip_N and Ip_C are 37 and 43%, respectively, to those of human SDH2 (Table 2), and the Ip_N and Ip_C domains contain all amino acid residues responsible for binding of iron-sulfur clusters and ubiquinone (12, 13, 30) (Fig. 4). Such a heterodimeric Ip subunit can be found in *T. brucei* (31), *T. cruzi*, *L. major*, *L. infantum*, and *L. brasiliensis* (Tables 2), which belong to the order Trypanosomatida. Thus we named these subunits as $SDH2_N$ and $SDH2_C$, respectively.

Splitting of mitochondrial membrane proteins has been reported for cytochrome *c* oxidase CoxII in Apicomplexa and Chlorophyceae (32, 33), and ATP synthase α subunit in *Leishmania tarentolae* and *T. brucei* (34, 35). The former occurs at the gene level and the latter by post-translational cleavage. Sequence analysis indicates that heterodimeric SDH2 and CoxII have emerged from gene duplication followed by degeneration of the N- or C-terminal half of the duplication products. Conserved domains in degenerated duplicons, which have arisen from mitochondrion-to-nucleus transfer of the duplicated genes (32, 33, 36), must retain the potential for protein-protein interactions and constitute a heterodimeric functional subunit by trans-complementation.

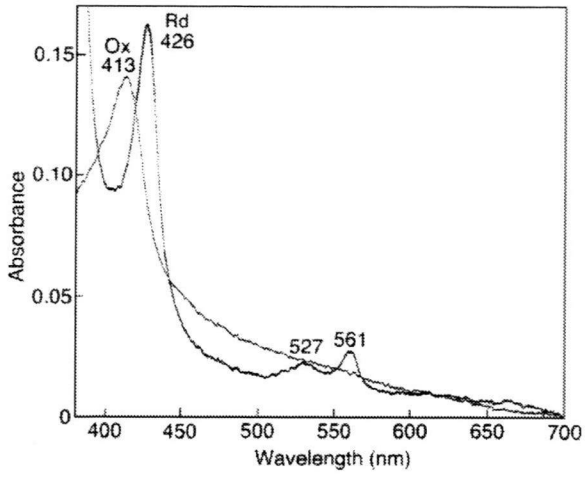

FIGURE 6. **Visible absorption spectra of *T. cruzi* Complex II.** Purified Complex II was desalted by ultrafiltration and diluted with 0.1 M sodium phosphate, pH 7.2, containing 0.1% SML at a final concentration of 0.06 mg/ml. Absorption spectra of the air-oxidized (*Ox, thin line*) and dithionite-reduced (*Rd, thick line*) forms were recorded at room temperature with UV-2400 spectrophotometer (Shimadzu Corp., Kyoto, Japan).

Membrane Anchor Subunits—Membrane anchor subunits in protist enzymes are highly divergent from bacterial and mammalian counterparts and difficult to find with conventional BLAST programs. We identified candidates for *T. cruzi* SDH3 and SDH4 by the presence of the quinone/heme-binding motifs "$RPX_{16}SX_2HR$ (SDH3 helix I)" and "$HX_{10}DY$ (SDH4 helix V)," respectively, present in membrane anchor subunits. In Complex II, Trp^{164} in SDH2 (Fig. 4) and Tyr^{83} in the SDH4 $HX_{10}DY$ motif (Fig. 5*B*) (*E. coli* numbering) could hydrogen bond to the O-1 atom of ubiquinone and contribute to the binding affinity (12, 37). Arg^{31} in the SDH3 SX_2HR motif (Fig. 5*A*) and Asp^{82} in the SDH4 $HX_{10}DY$ motif are in close proximity to ubiquinone and could interact with Tyr^{83} (37). Ser^{27} in the SDH3 SX_2HR motif has been shown to be essential for quinone binding (38) and is a candidate for hydrogen bonding to the O-4 atom of ubiquinone (30). The first arginine (Arg^9 in *E. coli* SDH3) in the $RPX_{16}SX_3R$ motif is in the vicinity of Glu^{186} in SDH1 and Asp^{106} in SDH2 and may play a structural role by making a hydrogen bond network.

In *T. cruzi*, SDH3 has the "$RPX_{11}SX_2HR$ motif in front of the predicted transmembrane helix I and lacks transmembrane helices II and III. However, sequence alignment suggests the presence of the alternative motif "$TX_2SR/(T)$" in the Trypanosomatida (Fig. 5*A*). In mitochondrial Complex II, protoheme IX is ligated by two His residues in the second transmembrane helix of SDH3 ("$HX_{10}D$" motif) and SDH4 ("$HX_{10}DY$" motif). A heme ligand in helix II (His^{84} in *E. coli* SDH3) may be substituted by a nearby histidine in the quinone-binding motif "SX_2HR" (39). In contrast, SDH4 lacks helix IV and appears to interact with heme and ubiquinone with the $HX_{10}DY$ motif. As in rice SDH4 (GenBank™ accession number NP_001045324), the heme ligand His is substituted by Gln in *T. brucei* SDH4. The presence of a bound heme or an alternative ligand in *T.*

brucei SDH4 needs to be tested in future studies. It is also possible that trypanosomatid-specific subunits could be assembled as a jigsaw puzzle-like membrane anchor.

Spectroscopic Properties of T. cruzi Complex II—Pyridine ferrohemochrome analysis showed that *T. cruzi* Complex II binds a stoichiometric amount of protoheme IX (0.85 heme/monomer of enzyme) indicating that monomer enzyme complex contains one heme. At room temperature, the air-oxidized and fully reduced forms of the purified enzyme showed peaks at 413 and 426, 527, and 561 nm, respectively (Fig. 6). Peak positions are similar to those reported for Complex II from *E. coli* (40), adult *A. suum* (41), and bovine (42, 43), where heme is ligated via histidine in the second helices of SDH3 and SDH4. Although heme has an important role in the assembly of Complex II, it is not essential for the reduction of ubiquinones (43, 44).

Enzymatic Properties of T. cruzi Complex II—We examined SQR activity of the purified enzyme and found the difference in apparent K_m values between Q_1 (33.9 ± 3.6 μM) and Q_2 (18.8 ± 6.4 μM) (Fig. 7), indicating that the 6-polyprenyl group of ubiquinone contributes to the binding affinity. The apparent V_{max} value of the *T. cruzi* Complex II was rather constant, 11.9 ± 2.2 for Q_1 and 11.5 ± 0.4 Q_2 units/mg proteins, respectively, and one-fourth of those reported for bovine and *E. coli* enzymes (45, 46). This is not surprising because *T. cruzi* complex II has about 2–3 times more proteins than the other enzymes. K_m values for ubiquinone and succinate (18.8 ± 6.4 μM (Q_2) and 1.48 ± 0.17 mM, respectively) were higher than 0.3 and 130 μM, respectively, of bovine enzyme (45), and 2 and 277 μM, respectively, of the *E. coli* enzyme (46, 47). Notably, the K_m value for succinate was comparable with 610 μM in adult *A. suum* (10), which expresses the stage-specific Complex II as quinol:fumarate reductase under hypoxic habitats in host organisms.

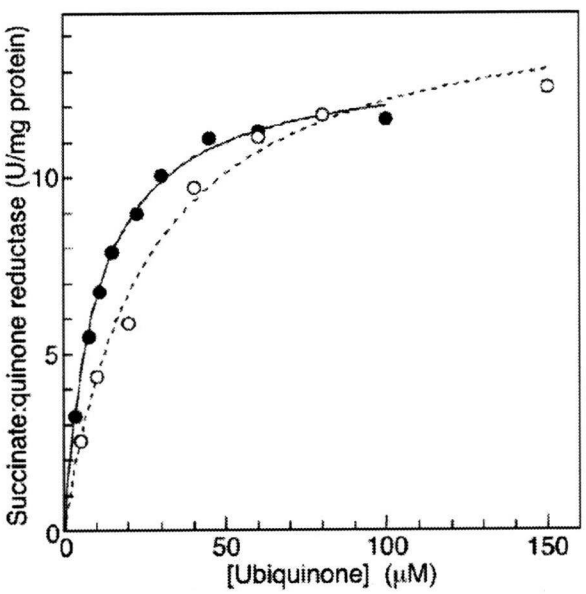

FIGURE 7. **Kinetic analysis of succinate-quinone reductase activity.** Succinate:ubiquinone reductase activity of the purified Complex II was determined with Q_1 (○) and Q_2 (●) at a protein concentration of 1.25 μg/ml in the presence of 10 mM sodium succinate. Data were fitted with the Michaelis-Menten equation using KaleidaGraph, and apparent K_m and V_{max} values were 30.3 ± 4.3 μM and 14.0 ± 1.2 units/mg protein, respectively, for Q_1 and 12.4 ± 0.7 μM and 11.9 ± 0.3 units/mg protein, respectively, for Q_2.

Then we examined effects of inhibitors for binding sites of quinones and dicarboxylates on SQR activity. Atpenin A5, a potent inhibitor for Complex II, inhibited the *T. cruzi* enzyme with the IC_{50} value of 6.4 ± 2.4 μM, which is 3 orders of magnitude higher than that of bovine Complex II (4 nM) (48). Furthermore, carboxin, 2-theonyltrifluoroacetone, plumbagin, and 2-heptyl-4-hydroxyquinoline *N*-oxide were ineffective (100 μM < IC_{50}). Structural divergence in trypanosomatid SDH3 and SDH4 could be the cause for lower binding affinities for both quinones and inhibitors. In addition, we found for the dicarboxylate-binding site that the IC_{50} value for malonate (40 μM) was much higher than the K_i value for bovine Complex II (1.3 μM) (45).

Structure of Trypanosomatid Complex II—To the best of our knowledge, this is the first report on the isolation of protist Complex II. *T. cruzi* Complex II has unusual subunit organization with six each of hydrophilic and hydrophobic subunits. Such a supramolecular structure and heterodimeric SDH2 ($SDH2_N$ and $SDH2_C$) are conserved in the Trypanosomatida. Furthermore, SDH1, $SDH2_N$, $SDH2_C$, SDH3, SDH4, and SDH8–SDH10 can be identified in the ongoing genome projects on the evolutionary relatives, the photosynthetic free-living *Euglena gracilis*, and the nonphotosynthetic euglenoid *Astasia longa* in the Euglenida. Thus a part of these features are common in the Euglenozoa, a divergent lineage of eukaryotes (Fig. 8).

Accumulation of noncatalytic subunits through expanding the protein interaction network could be a driving force for protein evolution. Structural and catalytic features are unique, and thus this enzyme could be a potential target for novel chemotherapeutic agents for trypanosomiasis and leishmaniasis.

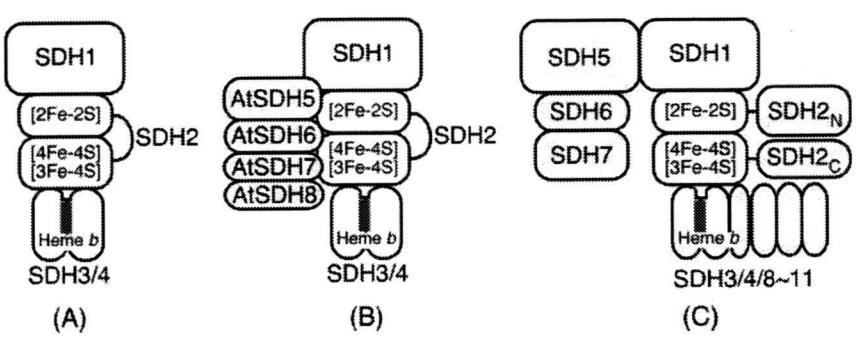

FIGURE 8. **Subunit organization of Complex II.** *A*, common four-subunit Complex II (*e.g.* mammals, *E. coli*); *B*, eight-subunit Complex II in plants (*e.g. A. thaliana*); and *C*, 12-subunit Complex II in the Trypanosomatida. Noncatalytic subunits and domains are shown in *yellow* and heme in *red*.

Conclusion—The parasitic protist *T. brucei* is a gold mine where unprecedented biological phenomena like RNA editing and trans-splicing in mitochondria were originally discovered. It was found recently in *Diplonema papillatum*, a free-living evolutionary cousin,

that mature mRNA for cytochrome *c* oxidase CoxI was assembled from nine gene fragments by a jigsaw puzzle mechanism (49). From a characterization of Complex II from *T. cruzi*, we revealed a novel supramolecular organization, which is conserved in the Trypanosomatida.

Parasites have exploited unique energy metabolic pathways as adaptations to their natural habitats within their hosts (50, 51). In fact, the respiratory systems of parasites typically show greater diversity in electron transfer pathways than those of host animals. As shown in this study, such is also the case with Complex II, which is a well known marker enzyme of mitochondria. Studies on the role of supramolecular Complex II in adaptation of trypanosomatids is now underway in our laboratory.

Acknowledgments—We thank Drs. J. L. Concepcion (Universidad de Los Andes, Merida-Venezuela) and T. Nara (Juntendo University) for kind advice; and Drs. M. Matsuzaki (University of Tokyo), T. Hashimoto (University of Tsukuba), G. Cecchini (University of California San Francisco), and M. Müller (Rockefeller University) for critical reading of the manuscript.

REFERENCES

1. World Health Organization (2007) *Report of the First Meeting of WHO Strategic and Technical Advisory Group on Neglected Tropical Diseases*, pp. 1–26, Geneva, Switzerland
2. Berriman, M., Ghedin, E., Hertz-Fowler, C., Blandin, G., Renauld, H., Bartholomeu, D. C., Lennard, N. J., Caler, E., Hamlin, N. E., Haas, B., Bohme, U., Hannick, L., Aslett, M. A., Shallom, J., Marcello, L., Hou, L., Wickstead, B., Alsmark, U. C., Arrowsmith, C., Atkin, R. J., Barron, A. J., Bringaud, F., Brooks, K., Carrington, M., Cherevach, I., Chillingworth, T. J., Churcher, C., Clark, L. N., Corton, C. H., Cronin, A., Davies, R. M., Doggett, J., Djikeng, A., Feldblyum, T., Field, M. C., Fraser, A., Goodhead, I., Hance, Z., Harper, D., Harris, B. R., Hauser, H., Hostetler, J., Ivens, A., Jagels, K., Johnson, D., Johnson, J., Jones, K., Kerhornou, A. X., Koo, H., Larke, N., Landfear, S., Larkin, C., Leech, V., Line, A., Lord, A., Macleod, A., Mooney, P. J., Moule, S., Martin, D. M., Morgan, G. W., Mungall, K., Norbertczak, H., Ormond, D., Pai, G., Peacock, C. S., Peterson, J., Quail, M. A., Rabbinowitsch, E., Rajandream, M. A., Reitter, C., Salzberg, S. L., Sanders, M., Schobel, S., Sharp, S., Simmonds, M., Simpson, A. J., Tallon, L., Turner, C. M., Tait, A., Tivey, A. R., Van Aken, S., Walker, D., Wanless, D., Wang, S., White, B., White, O., Whitehead, S., Woodward, J., Wortman, J., Adams, M. D., Embley, T. M., Gull, K., Ullu, E., Barry, J. D., Fairlamb, A. H., Opperdoes, F., Barrell, B. G., Donelson, J. E., Hall, N., Fraser, C. M., Melville, S. E., and El-Sayed, N. M. (2005) *Science* **309,** 416–422
3. Cazzulo, J. J. (1994) *J. Bioenerg. Biomembr.* **26,** 157–165
4. Besteiro, S., Barrett, M. P., Riviere, L., and Bringaud, F. (2005) *Trends Parasitol.* **21,** 185–191
5. Bringaud, F., Riviere, L., and Coustou, V. (2006) *Mol. Biochem. Parasitol.* **149,** 1–9
6. Takashima, E., Inaoka, D. K., Osanai, A., Nara, T., Odaka, M., Aoki, T., Inaka, K., Harada, S., and Kita, K. (2002) *Mol. Biochem. Parasitol.* **122,** 189–200
7. Van Hellemond, J. J., Opperdoes, F. R., and Tielens, A. G. (1998) *Proc. Natl. Acad. Sci. U. S. A.* **95,** 3036–3041
8. Harington, J. S. (1961) *Parasitology* **51,** 309–318
9. Roos, M. H., and Tielens, A. G. (1994) *Mol. Biochem. Parasitol.* **66,** 273–281
10. Saruta, F., Kuramochi, T., Nakamura, K., Takamiya, S., Yu, Y., Aoki, T., Sekimizu, K., Kojima, S., and Kita, K. (1995) *J. Biol. Chem.* **270,** 928–932
11. Cecchini, G. (2003) *Annu. Rev. Biochem.* **72,** 77–109
12. Yankovskaya, V., Horsefield, R., Tornroth, S., Luna-Chavez, C., Miyoshi, H., Leger, C., Byrne, B., Cecchini, G., and Iwata, S. (2003) *Science* **299,** 700–704
13. Sun, F., Huo, X., Zhai, Y., Wang, A., Xu, J., Su, D., Bartlam, M., and Rao, Z. (2005) *Cell* **121,** 1043–1057
14. Huang, L. S., Sun, G., Cobessi, D., Wang, A. C., Shen, J. T., Tung, E. Y., Anderson, V. E., and Berry, E. A. (2006) *J. Biol. Chem.* **281,** 5965–5972
15. El-Sayed, N. M., Myler, P. J., Bartholomeu, D. C., Nilsson, D., Aggarwal, G., Tran, A. N., Ghedin, E., Worthey, E. A., Delcher, A. L., Blandin, G., Westenberger, S. J., Caler, E., Cerqueira, G. C., Branche, C., Haas, B., Anupama, A., Arner, E., Aslund, L., Attipoe, P., Bontempi, E., Bringaud, F., Burton, P., Cadag, E., Campbell, D. A., Carrington, M., Crabtree, J., Darban, H., da Silveira, J. F., de Jong, P., Edwards, K., Englund, P. T., Fazelina, G., Feldblyum, T., Ferella, M., Frasch, A. C., Gull, K., Horn, D., Hou, L., Huang, Y., Kindlund, E., Klingbeil, M., Kluge, S., Koo, H., Lacerda, D., Levin, M. J., Lorenzi, H., Louie, T., Machado, C. R., McCulloch, R., McKenna, A., Mizuno, Y., Mottram, J. C., Nelson, S., Ochaya, S., Osoegawa, K., Pai, G., Parsons, M., Pentony, M., Pettersson, U., Pop, M., Ramirez, J. L., Rinta, J., Robertson, L., Salzberg, S. L., Sanchez, D. O., Seyler, A., Sharma, R., Shetty, J., Simpson, A. J., Sisk, E., Tammi, M. T., Tarleton, R., Teixeira, S., Van Aken, S., Vogt, C., Ward, P. N., Wickstead, B., Wortman, J., White, O., Fraser, C. M., Stuart, K. D., and Andersson, B. (2005) *Science* **309,** 409–415
16. Ivens, A. C., Peacock, C. S., Worthey, E. A., Murphy, L., Aggarwal, G., Berriman, M., Sisk, E., Rajandream, M. A., Adlem, E., Aert, R., Anupama, A., Apostolou, Z., Attipoe, P., Bason, N., Bauser, C., Beck, A., Beverley, S. M., Bianchettin, G., Borzym, K., Bothe, G., Bruschi, C. V., Collins, M., Cadag, E., Ciarloni, L., Clayton, C., Coulson, R. M., Cronin, A., Cruz, A. K., Davies, R. M., De Gaudenzi, J., Dobson, D. E., Duesterhoeft, A., Fazelina, G., Fosker, N., Frasch, A. C., Fraser, A., Fuchs, M., Gabel, C., Goble, A., Goffeau, A., Harris, D., Hertz-Fowler, C., Hilbert, H., Horn, D., Huang, Y., Klages, S., Knights, A., Kube, M., Larke, N., Litvin, L., Lord, A., Louie, T., Marra, M., Masuy, D., Matthews, K., Michaeli, S., Mottram, J. C., Muller-Auer, S., Munden, H., Nelson, S., Norbertczak, H., Oliver, K., O'Neil, S., Pentony, M., Pohl, T. M., Price, C., Purnelle, B., Quail, M. A., Rabbinowitsch, E., Reinhardt, R., Rieger, M., Rinta, J., Robben, J., Robertson, L., Ruiz, J. C., Rutter, S., Saunders, D., Schafer, M., Schein, J., Schwartz, D. C., Seeger, K., Seyler, A., Sharp, S., Shin, H., Sivam, D., Squares, R., Squares, S., Tosato, V., Vogt, C., Volckaert, G., Wambutt, R., Warren, T., Wedler, H., Woodward, J., Zhou, S., Zimmermann, W., Smith, D. F., Blackwell, J. M., Stuart, K. D., Barrell, B., and Myler, P. J. (2005) *Science* **309,** 436–442
17. Bourguignon, S. C., Mello, C. B., Santos, D. O., Gonzalez, M. S., and Souto-Padron, T. (2006) *Acta Trop.* **98,** 103–109
18. Concepcion, J. L., Chataing, B., and Dubourdieu, M. (1999) *Comp. Biochem. Physiol.* **122,** 211–222
19. Matsudaira, P. (1987) *J. Biol. Chem.* **262,** 10035–10038
20. Rosenfeld, J., Capdevielle, J., Guillemot, J. C., and Ferrara, P. (1992) *Anal. Biochem.* **203,** 173–179
21. Brusca, J. S., and Radolf, J. D. (1994) *Methods Enzymol.* **228,** 182–193
22. Wittig, I., Karas, M., and Schagger, H. (2007) *Mol. Cell. Proteomics* **6,** 1215–1225
23. Sabar, M., Balk, J., and Leaver, C. J. (2005) *Plant J.* **44,** 893–901
24. Berry, E. A., and Trumpower, B. L. (1987) *Anal. Biochem.* **161,** 1–15
25. Larkin, M. A., Blackshields, G., Brown, N. P., Chenna, R., McGettigan, P. A., McWilliam, H., Valentin, F., Wallace, I. M., Wilm, A., Lopez, R., Thompson, J. D., Gibson, T. J., and Higgins, D. G. (2007) *Bioinformatics (Oxf.)* **23,** 2947–2948
26. Schagger, H., and Pfeiffer, K. (2000) *EMBO J.* **19,** 1777–1783
27. Millar, A. H., Eubel, H., Jansch, L., Kruft, V., Heazlewood, J. L., and Braun, H. P. (2004) *Plant Mol. Biol.* **56,** 77–90
28. Eubel, H., Heinemeyer, J., and Braun, H. P. (2004) *Plant Physiol.* **134,** 1450–1459
29. Eubel, H., Heinemeyer, J., Sunderhaus, S., and Braun, H. P. (2004) *Plant Physiol. Biochem.* **42,** 937–942
30. Horsefield, R., Yankovskaya, V., Sexton, G., Whittingham, W., Shiomi, K., Omura, S., Byrne, B., Cecchini, G., and Iwata, S. (2006) *J. Biol. Chem.* **281,** 7309–7316
31. Allen, J. W., Ginger, M. L., and Ferguson, S. J. (2004) *Biochem. J.* **383,** 537–542
32. Funes, S., Davidson, E., Reyes-Prieto, A., Magallon, S., Herion, P., King, M. P., and Gonzalez-Halphen, D. (2002) *Science* **298,** 2155

33. Waller, R. F., and Keeling, P. J. (2006) *Gene (Amst.)* **383,** 33–37
34. Williams, N., and Frank, P. H. (1990) *Mol. Biochem. Parasitol.* **43,** 125–132
35. Nelson, R. E., Aphasizheva, I., Falick, A. M., Nebohacova, M., and Simpson, L. (2004) *Mol. Biochem. Parasitol.* **135,** 221–224
36. Adams, K. L., Rosenblueth, M., Qiu, Y. L., and Palmer, J. D. (2001) *Genetics* **158,** 1289–1300
37. Tran, Q. M., Rothery, R. A., Maklashina, E., Cecchini, G., and Weiner, J. H. (2006) *J. Biol. Chem.* **281,** 32310–32317
38. Yang, X., Yu, L., He, D., and Yu, C. A. (1998) *J. Biol. Chem.* **273,** 31916–31923
39. Maklashina, E., Rothery, R. A., Weiner, J. H., and Cecchini, G. (2001) *J. Biol. Chem.* **276,** 18968–18976
40. Kita, K., Vibat, C. R., Meinhardt, S., Guest, J. R., and Gennis, R. B. (1989) *J. Biol. Chem.* **264,** 2672–2677
41. Takamiya, S., Furushima, R., and Oya, H. (1986) *Biochim. Biophys. Acta* **848,** 99–107
42. Tushurashvili, P. R., Gavrikova, E. V., Ledenev, A. N., and Vinogradov, A. D. (1985) *Biochim. Biophys. Acta* **809,** 145–159
43. Tran, Q. M., Rothery, R. A., Maklashina, E., Cecchini, G., and Weiner, J. H. (2007) *Proc. Natl. Acad. Sci. U. S. A.* **104,** 18007–18012
44. Oyedotun, K. S., Sit, C. S., and Lemire, B. D. (2007) *Biochim. Biophys. Acta* **1767,** 1436–1445
45. Grivennikova, V. G., Gavrikova, E. V., Timoshin, A. A., and Vinogradov, A. D. (1993) *Biochim. Biophys. Acta* **1140,** 282–292
46. Maklashina, E., and Cecchini, G. (1999) *Arch. Biochem. Biophys.* **369,** 223–232
47. Miyadera, H., Hiraishi, A., Miyoshi, H., Sakamoto, K., Mineki, R., Murayama, K., Nagashima, K. V., Matsuura, K., Kojima, S., and Kita, K. (2003) *Eur. J. Biochem.* **270,** 1863–1874
48. Miyadera, H., Shiomi, K., Ui, H., Yamaguchi, Y., Masuma, R., Tomoda, H., Miyoshi, H., Osanai, A., Kita, K., and Omura, S. (2003) *Proc. Natl. Acad. Sci. U. S. A.* **100,** 473–477
49. Marande, W., and Burger, G. (2007) *Science* **318,** 415
50. Kita, K., and Takamiya, S. (2002) *Adv. Parasitol.* **51,** 95–131
51. Tielens, A. G., Rotte, C., van Hellemond, J. J., and Martin, W. (2002) *Trends Biochem. Sci.* **27,** 564–572
52. Krogh, A., Larsson, B., von Heijne, G., and Sonnhammer, E. L. L. (2001) *J. Mol. Biol.* **305,** 567–580
53. Mitaku, S., Hirokawa, T., and Tsuji, T. (2002) *Bioinformatics* **18,** 608–616

Acta Crystallographica Section F
Structural Biology and Crystallization Communications
ISSN 1744-3091

Crystallization of mitochondrial rhodoquinol-fumarate reductase from the parasitic nematode *Ascaris suum* with the specific inhibitor flutolanil

Arihiro Osanai,[a] Shigeharu Harada,[b] Kimitoshi Sakamoto,[a]* Hironari Shimizu,[a] Daniel Ken Inaoka[a] and Kiyoshi Kita[a]

[a]Department of Biomedical Chemistry, Graduate School of Medicine, University of Tokyo, 7-3-1 Hongo, Bunkyo-ku, Tokyo 113-0033, Japan, and [b]Department of Applied Biology, Graduate School of Science and Technology, Kyoto Institute of Technology, Sakyo-ku, Kyoto 606-8585, Japan

Correspondence e-mail: sakamok@m.u-tokyo.ac.jp

Received 2 June 2009
Accepted 8 August 2009

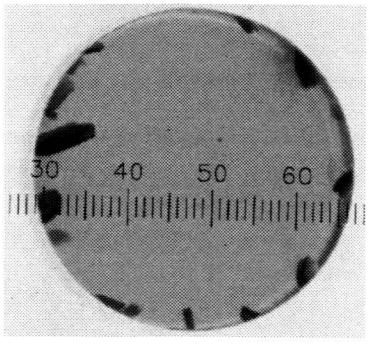

In adult *Ascaris suum* (roundworm) mitochondrial membrane-bound complex II acts as a rhodoquinol-fumarate reductase, which is the reverse reaction to that of mammalian complex II (succinate-ubiquinone reductase). The adult *A. suum* rhodoquinol-fumarate reductase was crystallized in the presence of octaethyleneglycol monododecyl ether and *n*-dodecyl-β-D-maltopyranoside in a 3:2 weight ratio. The crystals belonged to the orthorhombic space group $P2_12_12_1$, with unit-cell parameters a = 123.75, b = 129.08, c = 221.12 Å, and diffracted to 2.8 Å resolution using synchrotron radiation. The presence of two molecules in the asymmetric unit (120 kDa × 2) gives a crystal volume per protein mass (V_M) of 3.6 Å^3 Da^{-1}.

1. Introduction

In parasites, fumarate plays an important role in redox homeostasis. The parasitic protozoan *Trypanosoma cruzi* utilizes bacterial-type dihydroorotate dehydrogenase (TcDHOD), which is the fourth enzyme in the pyrimidine-biosynthesis pathway and catalyzes the oxidation of dihydroorotate and the reduction of fumarate to succinate. We have elucidated the catalytic mechanisms of these sequential reactions by determination of the three-dimensional structures of TcDHOD in the ligand-free form and in complex with the substrates (dihydroorotate and fumarate), product (orotate and succinate) and inhibitor (oxonate) at atomic resolution (Inaoka *et al.*, 2008).

In parasitic helminths, fumarate is the terminal electron acceptor of the anaerobic respiratory chain, which is essential for the survival of the parasites in the host (Kita & Takamiya, 2002). Complex II catalyzes fumarate reduction in anaerobic respiration and functions as a terminal oxidase. In eukaryotes, complex II (succinate-ubiquinone reductase in aerobic respiration; SQR) is located in the inner mitochondrial membrane and is generally composed of four polypeptides. The flavoprotein (Fp) subunit is the largest, with an approximate molecular mass of 70 kDa, and contains flavin adenine dinucleotide (FAD) as a prosthetic group. Complex II contains a relatively hydrophilic catalytic region formed by the Fp subunit and an iron–sulfur cluster (Ip) subunit, which has a molecular mass of approximately 30 kDa. The remaining subunits comprise cytochrome *b*, which contains a haem *b*. Cytochrome *b* is composed of two hydrophobic membrane-anchoring polypeptide subunits, namely a 15 kDa large subunit (CybL) and a 13 kDa small subunit (CybS). These cytochrome *b* subunits are necessary for the interaction of complex II with hydrophobic membrane-associated quinones such as ubiquinone (UQ) and rhodoquinone (RQ).

Our recent study on the respiratory chain of the parasitic nematode *Ascaris suum* has shown that the mitochondrial NADH-fumarate reductase system plays an important role in the anaerobic energy metabolism of adult parasites inhabiting hosts and that they undergo unique developmental changes during their life cycle (Kita & Takamiya, 2002; Iwata *et al.*, 2008). In anaerobic metabolism by *A. suum* mitochondria, the transfer of a reducing equivalent from NADH to the low-potential RQ is conducted by the NADH–RQ reductase complex (complex I). This pathway ends with the production of succinate by the rhodoquinol-fumarate reductase (QFR) activity of complex II. Electron transfer from NADH to fumarate is

doi:10.1107/S1744309109031352

coupled to site I phosphorylation of complex I *via* the generation of a proton gradient. The difference in redox potential between the NAD^+/NADH couple (E'_m = −320 mV) and the fumarate/succinate couple (E'_m = +30 mV) is sufficient to drive ATP synthesis.

The anaerobic NADH-fumarate reductase system is found not only in nematodes but also in bacteria and many other parasites and is a promising target for chemotherapy (Omura *et al.*, 2001; Tielens *et al.*, 2002; Matsumoto *et al.*, 2008). The most potent inhibitor of complex II, atpenin A5, was found during screening for inhibitors of *A. suum* complex II (Miyadera *et al.*, 2003). However, the mammalian complex II is much more sensitive to atpenin A5 than the *A. suum* enzyme. By further screening, we have found that flutolanil, a commercially available fungicide (Ito *et al.*, 2004), specifically inhibits the *A. suum* complex II. Therefore, we have taken flutolanil as a lead compound for structure-based drug design. In the current study, we have purified, crystallized and performed preliminary X-ray diffraction studies on the adult *A. suum* QFR.

2. Methods

2.1. Purification

Mitochondria were prepared from the muscle of adult *A. suum* as described by Takamiya *et al.* (1984), except that Chappell–Perry medium (100 m*M* KCl, 50 m*M* Tris–HCl pH 7.4, 1 m*M* ATP, 5 m*M* $MgSO_4$ and 1 m*M* EDTA; Ernster & Nordenbrand, 1967) was used instead of MSE medium (210 m*M* mannitol, 70 m*M* sucrose and 0.1 m*M* EDTA). The QFR was solubilized from adult *A. suum* mitochondria in 1.0%(*w*/*v*) sucrose monolaurate (Dojindo) and purified in the presence of 0.1%(*w*/*v*) sucrose monolaurate. *A. suum* mitochondria (1 g protein) were homogenized in 500 ml buffer *A* (10 m*M* Tris–HCl pH 7.5, 1 m*M* sodium malonate) containing 1.0%(*w*/*v*) sucrose monolaurate. After incubating the mixture for 30 min at 277 K, it was centrifuged for 1 h at 200 000*g*. The clear reddish-brown supernatant containing the solubilized QFR was applied onto a GE Healthcare DEAE Sepharose FF column (2.6 × 24 cm) pre-equilibrated with buffer *A* containing 0.1%(*w*/*v*) sucrose monolaurate. After washing the column with the same buffer, the QFR was eluted with 2400 ml of the buffer containing a linear gradient of 0.0–0.3 *M* NaCl. Fractions containing the QFR, which started to elute at approximately 0.1 *M* NaCl, were pooled and adjusted to 0.15 g ml^{-1} polyethylene glycol 3350 (Hampton Research) to precipitate the QFR. The mixture was centrifuged for 20 min at 15 000*g* and the precipitate was dissolved in buffer *A* containing 0.1%(*w*/*v*) sucrose monolaurate. The QFR was then further loaded onto a GE Healthcare Source 15Q column (1.6 × 10 cm) and eluted with 400 ml of buffer containing a linear gradient of 0–0.3 *M* NaCl. Fractions containing pure QFR as judged by SDS–PAGE (Fig. 1) were pooled. The purified QFR was then precipitated by adding solid polyethylene glycol (PEG) 3350 to 0.15 g ml^{-1} and stored at 193 K.

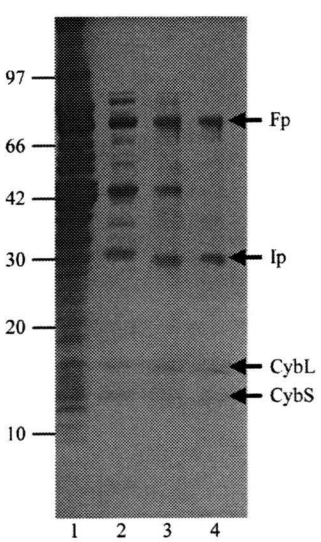

Figure 1
Purity of *A. suum* QFR at different stages of purification. Samples were separated by SDS–PAGE and the gel was stained with Coomassie Blue. The positions of molecular-weight markers are indicated on the left (in kDa) and the four subunits of *A. suum* QFR (Fp, flavoprotein subunit; Ip, iron–sulfur cluster subunit; CybL, cytochrome *b* large subunit; CybS, cytochrome *b* small subunit) are labelled on the right. Lane 1, whole mitochondria; lane 2, supernatant obtained after ultracentrifugation of the detergent extract; lane 3, pooled fractions from the DEAE Sepharose FF column; lane 4, pooled fractions from the Source 15Q column.

2.2. Crystallization

Conditions for crystallizing the *A. suum* QFR were screened using Crystal Screen (Jancarik & Kim, 1991) and Crystal Screen II (Hampton Research). Crystallization by hanging-drop vapour diffusion was carried out using 96-well CrystalClear Strips (Hampton Research). A droplet containing equal volumes of approximately 20 mg ml^{-1} QFR in buffer *A* containing detergent and reservoir solution was equilibrated against 100 µl reservoir solution.

Aggregates of microcrystals were observed at 293 K from reservoir solutions containing polyethylene glycols with medium molecular weights and 200 m*M* salts when octaethyleneglycol monododecyl ether (C12E8) was used as a detergent. Attempts to optimize the conditions by altering the PEG type (3350, 4000 and 6000), PEG concentration and pH and by using Additive Screen kits (Hampton Research) did not succeed in improving the crystallization. We therefore examined the effect of adding another detergent as an additive. 0.1 volume of detergent solution was added to a droplet of approximately 20 mg ml^{-1} QFR in buffer *A* containing 0.5%(*w*/*v*) C12E8 and an equal volume of reservoir solution and crystallization by hanging-drop vapour diffusion was carried out. After several days, small crystals (~10 µm; Fig. 2*a*) appeared at 293 K in drops from reservoir solutions composed of 14–18%(*w*/*v*) PEG 3350, 100 m*M* Tris–HCl pH 7.5–8.6, 200 m*M* NaCl and 1 m*M* sodium malonate when the drops included 0.3–0.5%(*w*/*v*) *n*-dodecyl-β-D-maltopyranoside (C12M). To determine the optimal ratio of C12E8 to C12M, crystallization was carried out using QFR dissolved in buffer *A* containing different concentrations of C12E8 and C12M. The best condition for crystallization (Fig. 2*b*) was achieved at a 3:2 C12E8:C12M weight ratio.

Crystals larger than 100 µm in size were grown by the microdialysis method as follows. The precipitate of the purified QFR stored at 193 K was dissolved in buffer *A* (approximately 10 mg ml^{-1}) containing 0.6%(*w*/*v*) C12E8, 0.4%(*w*/*v*) C12M and 200 m*M* NaCl. After incubation for 20 min on ice, the QFR was precipitated by adding an equal volume of 40%(*w*/*v*) PEG 3350. The precipitate obtained by centrifugation was dissolved in the same buffer, incubated for 20 min on ice and mixed with an equal volume of 40%(*w*/*v*) PEG 3350 to precipitate the QFR. This procedure was repeated several times in order to replace sucrose monolaurate with the added detergent. The precipitate was finally dissolved in buffer *A* containing 0.06%(*w*/*v*) C12E8, 0.04%(*w*/*v*) C12M and 0.2 *M* NaCl, giving an approximately 40 mg ml^{-1} QFR solution. After adding an equal volume of 23%(*w*/*v*) PEG 3350 to the QFR solution, undissolved materials were removed by centrifugation for 20 min at 20 000*g*. The supernatant was then sealed in a 5 µl microdialysis button and dialyzed against

reservoir solution containing 15.0%(*w*/*v*) PEG 3350, 100 m*M* Tris–HCl pH 8.4, 200 m*M* NaCl, 1 m*M* sodium malonate, 0.06%(*w*/*v*) C12E8 and 0.04%(*w*/*v*) C12M. Dark red plate-shaped crystals appeared within 24 h and grew to 100–200 µm after 2–3 d at 293 K (Fig. 2*c*).

X-ray diffraction data were collected on BL44XU at SPring-8 (Harima, Japan) and on BL-5A and NW12A at the Photon Factory (Tsukuba, Japan) by the rotation method. For X-ray diffraction experiments at 100 K, a QFR crystal mounted on a nylon loop was transferred successively to reservoir solution supplemented with 3.75, 7.5, 11.25 and 15% glycerol and was then frozen by rapid submergence in liquid nitrogen. Data were processed and scaled using *HKL*-2000 and *SCALEPACK* (Otwinowski & Minor, 1997).

3. Results and discussion

To obtain sufficient *A. suum* mitochondria for purification of the QFR, we slightly modified the standard protocol. Specifically, we used Chappell–Perry medium (Ernster & Nordenbrand, 1967) in place of the standard medium. This resulted in 0.95 mg mitochondria per gram of muscle and 0.3 µmol min^{-1} mg^{-1} mitochondrial succinate dehydrogenase activity, which represents a threefold increase in recovery and a fourfold increase in specific activity compared with the previous method (Takamiya *et al.*, 1984). Using this method, we obtained 7.5 mg pure enzyme (Fig. 1, lane 4) from 1 kg of adult *A. suum* muscle.

Because the success of membrane-protein crystallization strongly depends on which detergent is used, we tested a variety of commercially available nonionic detergents in the screening of crystallization conditions for the *A. suum* QFR. Aggregates of microcrystals were obtained under several crystallization conditions using the detergent C12E8, but we were unable to optimize the conditions. Instead, the optimal condition for producing crystals suitable for X-ray structure analysis was achieved when the sucrose monolaurate was exchanged for a 3:2 weight ratio of C12E8:C12M (Fig. 2*c*). Crystals grew to larger than 100 µm in 2–3 d by dialyzing QFR, which was dissolved in buffer *A* containing 11.5%(*w*/*v*) PEG 3350, 0.06%(*w*/*v*) C12E8, 0.04%(*w*/*v*) C12M and 200 m*M* NaCl, against reservoir solution containing 15.0%(*w*/*v*) PEG 3350, 100 m*M* Tris–HCl pH 8.4, 200 m*M* NaCl, 1 m*M* sodium malonate, 0.06%(*w*/*v*) C12E8 and 0.04%(*w*/*v*) C12M. Adding 11.5%(*w*/*v*) PEG 3350 to the QFR solution in advance prevented serious bubble formation in the microdialysis button, which was unfavourable for crystallization.

X-ray diffraction patterns were recorded from a single crystal at 100 K with an oscillation angle of 1.0° using a Bruker DIP-6040 imaging-plate detector on the BL44XU beamline at SPring-8. Analysis of the symmetry and the systematic absences in the recorded diffraction pattern indicated that the crystals belonged to the orthorhombic space group $P2_12_12_1$, with unit-cell parameters a = 123.75, b = 129.08, c = 221.12 Å. Assuming the presence of two QFR molecules (120 kDa × 2) in the asymmetric unit, the calculated Matthews coefficient V_M (Matthews, 1968) was 3.6 $Å^3$ Da^{-1}. A total of 587 189 observed reflections recorded on 180 images were merged to 75 372 unique reflections from 50.0 to 2.8 Å resolution.

During the screening of inhibitors, we found that flutolanil (Ito *et al.*, 2004), a commercially available fungicide, specifically inhibits *A. suum* SQR. The IC_{50} of flutolanil against *A. suum* and bovine SQR was 0.081 and 16 µ*M*, respectively, indicating that flutolanil is a promising lead compound for anthelminthics. To enable rational drug optimization, we prepared crystals of the *A. suum* QFR complexed with flutolanil by the soaking method. X-ray diffraction patterns were recorded at 100 K on 130 frames with an oscillation angle of 1° using an ADSC Quantum 315 CCD detector on NW12 at Photon Factory. A total of 54 964 unique reflections from 50.0 to 3.2 Å resolution were obtained. The data-collection and processing statistics are summarized in Table 1.

We attempted to solve the structure of the *A. suum* QFR by the molecular-replacement method using the *MOLREP* program (Navaza, 1994) as implemented within *CCP*4 (Collaborative Computational Project, Number 4, 1994) and the refined coordinates

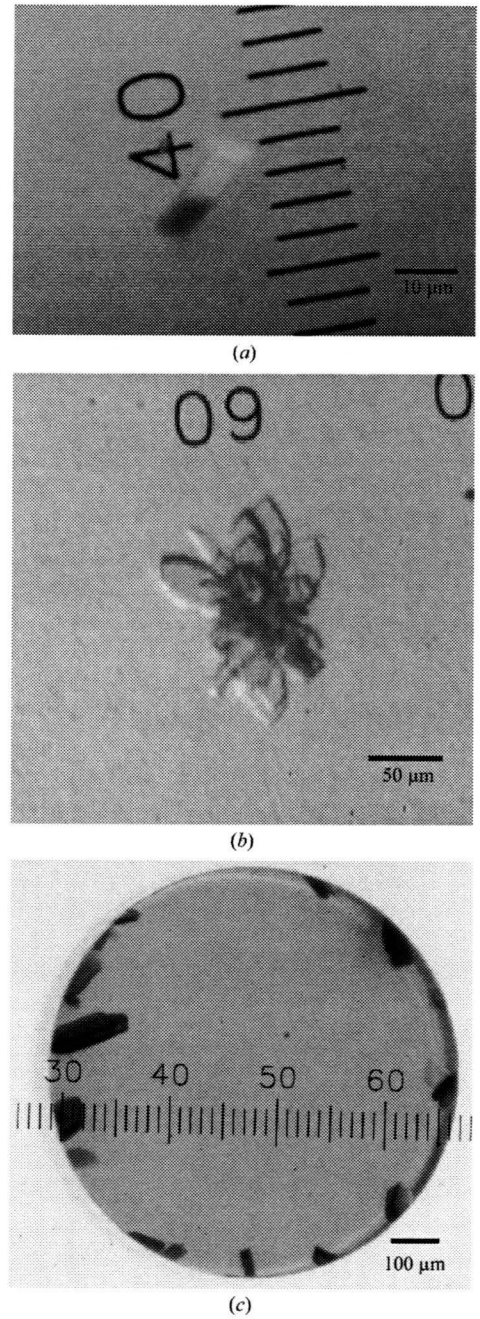

Figure 2
Typical crystals of *A. suum* QFR. Crystals of *A. suum* QFR obtained (*a*) by the hanging-drop vapour-diffusion method using C12E8 as the main detergent and C12M as the additive detergent, (*b*) using a 3:2 weight ratio of C12E8 and C12M and (*c*) after detergent exchange to the 3:2 C12E8:C12M mixture by microdialysis.

Table 1
Statistics of data collection and processing.

Values in parentheses are for the highest resolution shell.

	A. suum QFR	*A. suum* QFR with flutolanil
X-ray source	BL44XU (SPring-8)	NW12A (Photon Factory)
Wavelength (Å)	0.900	1.000
Space group	$P2_12_12_1$	$P2_12_12_1$
Unit-cell parameters		
a (Å)	123.75	124.31
b (Å)	129.08	131.63
c (Å)	221.12	222.53
Resolution range (Å)	50.0–2.8 (2.9–2.8)	50.0–3.20 (3.35–3.20)
No. of reflections	587189	207156
Unique reflections	75372	54964
Completeness (%)	89.2 (58.8)	93.9 (84.1)
R_{merge}† (%)	10.5 (36.6)	11.5 (40.0)
$I/\sigma(I)$	8.4 (3.5)	17.4 (1.6)

† $R_{merge} = \sum_{hkl}\sum_i |I_i(hkl) - \langle I(hkl)\rangle| / \sum_{hkl}\sum_i I_i(hkl)$.

of SQR from pig heart mitochondria (Sun *et al.*, 2005; PDB code 1zoy). The sequence identities between the pig and *A. suum* enzymes are 70.4, 68.3, 34.8 and 46.3% for the Fp, Ip, CybL and CybS subunits, respectively. Using X-ray diffraction data in the resolution range 15.0–2.8 Å collected from the flutolanil-free QFR crystal, a promising solution with two molecules per asymmetric unit was obtained and an *R* factor of 0.45 was achieved when the model was subsequently subjected to rigid-body refinement. Starting from the molecular-replacement solution, the structures of the flutolanil-free and flutolanil-bound forms of the *A. suum* QFR are currently being refined and electron density corresponding to bound flutolanil has been identified. The structures of the *A. suum* QFR together with those of the QFRs from *Wolinella succinogenes* (Lancaster *et al.*, 1999) and *Escherichia coli* (Iverson *et al.*, 1999) and the SQRs from *E. coli* (Yankovskaya *et al.*, 2003), pig heart mitochondria (Sun *et al.*, 2005) and avian heart mitochondria (Huang *et al.*, 2006) should help to clarify the structure–function relationships in complex II. In addition, the structure of the *A. suum* QFR complexed with flutolanil should provide information for the structure-based design of anthelminthics.

We are grateful to the staff of BL44XU at SPring-8 and the staff of NW12 and BL-5A at Photon Factory for their help with the collection of X-ray diffraction data. This work was supported in part by a grant from the Japan Aerospace Exploration Agency and by Grants-in-Aid for Scientific Research on Priority Areas from the 21st Century COE Program (F-3), for Creative Scientific Research and Targeted Proteins Research Program from the Japanese Ministry of Education, Culture, Sports, Science and Technology (180 73004, 18GS0314 and 1903610), and for Scientific Research (B) from the Japan Society for the Promotion of Science (18370042). DKI was a research fellow supported by the Japan Society for the Promotion of Science.

References

Collaborative Computational Project, Number 4 (1994). *Acta Cryst.* D**50**, 760–763.
Ernster, L. & Nordenbrand, K. (1967). *Methods Enzymol.* **10**, 86–94.
Huang, L. S., Sun, G., Cobessi, D., Wang, A. C., Shen, J. T., Tung, E. Y., Anderson, V. E. & Berry, E. A. (2006). *J. Biol. Chem.* **281**, 5965–5972.
Inaoka, D. K., Sakamoto, K., Shimizu, H., Shiba, T., Kurisu, G., Nara, T., Aoki, T., Kita, K. & Harada, S. (2008). *Biochemistry*, **47**, 10881–10891.
Ito, Y., Muraguchi, H., Seshime, Y., Oita, S. & Yanagi, S. O. (2004). *Mol. Genet. Genomics*, **272**, 328–335.
Iverson, T. M., Luna-Chaves, C., Cecchini, G. & Rees, D. C. (1999). *Science*, **284**, 1961–1966.
Iwata, F., Shinjyo, N., Amino, H., Sakamoto, K., Islam, M. K., Tsuji, N. & Kita, K. (2008). *Parasitol. Int.* **57**, 54–61.
Jancarik, J. & Kim, S.-H. (1991). *J. Appl. Cryst.* **24**, 409–411.
Kita, K. & Takamiya, S. (2002). *Adv. Parasitol.* **51**, 95–131.
Lancaster, C. R. D., Kröger, A., Auer, M. & Michel, H. (1999). *Nature (London)*, **402**, 377–385.
Matsumoto, J., Sakamoto, K., Shinjyo, N., Kido, Y., Yamamoto, N., Yagi, K., Miyoshi, H., Nonaka, N., Katakura, K., Kita, K. & Oku, Y. (2008). *Antimicrob. Agents. Chemother.* **52**, 164–170.
Matthews, B. W. (1968). *J. Mol. Biol.* **33**, 491–497.
Miyadera, H., Shiomi, K., Ui, H., Yamaguchi, Y., Masuma, R., Tomoda, H., Miyoshi, H., Osanai, A., Kita, K. & Omura, S. (2003). *Proc. Natl Acad. Sci. USA*, **100**, 473–477.
Navaza, J. (1994). *Acta Cryst.* A**50**, 157–163.
Omura, S. *et al.* (2001). *Proc. Natl Acad. Sci. USA*, **98**, 60–62.
Otwinowski, Z. & Minor, W. (1997). *Methods Enzymol.* **276**, 307–326.
Sun, F., Huo, X., Zhai, Y., Wang, A., Xu, J., Su, D., Bartlam, M. & Rao, Z. (2005). *Cell*, **121**, 1043–1057.
Takamiya, S., Furushima, R. & Oya, H. (1984). *Mol. Biochem. Parasitol.* **13**, 121–134.
Tielens, A. G. M., Rotte, C., van Hellemond, J. J. & Martin, W. (2002). *Trends Biochem. Sci.* **27**, 564–572.
Yankovskaya, V., Horsefield, R., Törnroth, S., Luna-Chaves, C., Miyoshi, H., Léger, C., Byrne, B., Cecchini, C. & Iwata, S. (2003). *Science*, **299**, 700–704.

Mitochondrion 9 (2009) 443–453

Contents lists available at ScienceDirect

Mitochondrion

journal homepage: www.elsevier.com/locate/mito

Identification of mitochondrial Complex II subunits SDH3 and SDH4 and ATP synthase subunits *a* and *b* in *Plasmodium* spp.

Tatsushi Mogi *, Kiyoshi Kita *

Department of Biomedical Chemistry, Graduate School of Medicine, The University of Tokyo, Hongo, Bunkyo-ku, Tokyo 113-0033, Japan

ARTICLE INFO

Article history:
Received 5 February 2009
Received in revised form 3 August 2009
Accepted 6 August 2009
Available online 12 August 2009

Keywords:
ATP synthase
Membrane anchor
Mitochondria
Plasmodium
Succinate dehydrogenase

ABSTRACT

While most protist mitochondrial enzymes could be identified in database, the membrane anchor subunits of Complex II and F_oF_1-ATP synthase of malaria parasites are not annotated. Based on the presence of structural fingerprints or proteomics data from other protists, here we present their candidates. In contrast to canonical subunits, *Plasmodium* Complex II anchors have two transmembrane helices and may coordinate heme *b via* Tyr in place of His. Transmembrane helix IV of ATP synthase subunit *a* lacks an essential Arg residue. Membrane anchors of *Plasmodium* Complex II and ATP synthase are divergent from orthologs and promising targets for new chemotherapeutics.

1. Introduction

Energy metabolism in the malaria parasites is quite different from that of mammalian hosts. The erythrocytic stage cells of *Plasmodium falciparum* cause mortality associated with malaria and are considered to rely on the incomplete oxidation of glucose, with the secretion of end products such as lactate and pyruvate (Sherman, 1998). Diversity in parasite metabolism and enzyme structures will facilitate the development of new antimalarials with novel targets and mechanisms against the drug-resistant strains of *Plasmodium* spp. (Hyde, 2005).

The *Plasmodium* mitochondrion of the erythrocytic stage parasites can oxidize NADH, glycerol-3-phosphate, succinate, dihydroorotate, and amino acids (Pro and Glu), but it is essentially acristate and apparently lacks oxidative phosphorylation and a functional tricarboxylic acid (TCA) cycle (Fry and Beesley, 1991; van Dooren et al., 2006). Pyruvate dehydrogenase is targeted to the apicoplast, not to the mitochondrion (Foth et al., 2005), and thus a major carbon flow from the cytoplasm to the mitochondrion of most eukaryotes is disconnected (Fig. 1). Fumarate inhibited the NADH-dependent reduction of cytochrome *c* and stimulated the oxidation of NADH, indicating an NADH–fumarate reductase pathway for the regeneration of NAD (Fry and Beesley, 1991). Recently, Painter et al. (2007) claimed for the erythrocytic stage cells of *P. falciparum* that the mitochondrial respiratory chain is required only for the regeneration of an oxidized form of ubiquinone, which serves as the electron acceptor for type 2 dihydroorotate dehydrogenase, an essential enzyme for pyrimidine biosynthesis. Thus, it is widely accepted that the majority of the erythrocytic stage parasite's ATP demand is met through glycolysis (Carlton et al., 2002).

In the insect vector stages, malaria parasites need to adapt to changes in available carbon sources from glucose in the mammalian blood to amino acids (e.g., Pro, Glu, His, and Ala (Henn et al., 1998)) in the mosquito hemolymph, which contains the disaccharide trehalose as a dominant sugar species. As amino acids are non-fermentable carbon sources, oxidative phosphorylation with the functional TCA cycle must take place in the insect stages. Proteomic profiling studies clearly demonstrated metabolic readjustments from the glycolytic pathway in the asexual stages trophozoites and schizonts to the TCA cycle in the salivary gland sporozoites (Lasonder et al., 2008). Metabolomic studies on the erythrocytic stage *P. falciparum* demonstrated that Gln was metabolized to L-malate *via* two pathways, the reductive carboxylation pathway through citrate yielding acetyl-CoA and the oxidative pathway through succinate yielding ATP and a precursor of heme biosynthesis (δ-aminolevulinic acid) (Olszewski, Rabinowitz, Llinás, personal communication) (Fig. 1). Thus, amino acids acquired from the mosquito hemolymph or the food vacuole of the erythrocytic stage parasites can be metabolized by entering the TCA cycle as 2-oxoglutarate *via* a bifurcated mechanism using

Abbreviations: FRD, fumarate reductase; SDH, succinate dehydrogenase; TCA, tricarboxylic acid; TM, transmembrane helix.

* Corresponding authors. Tel.: +81 3 5841 3526; fax: +81 3 5841 3444.
E-mail addresses: tmogi@m.u-tokyo.ac.jp (T. Mogi), kitak@m.u-tokyo.ac.jp (K. Kita).

1567-7249/$ - see front matter © 2009 Elsevier B.V. and Mitochondria Research Society. All rights reserved.
doi:10.1016/j.mito.2009.08.004

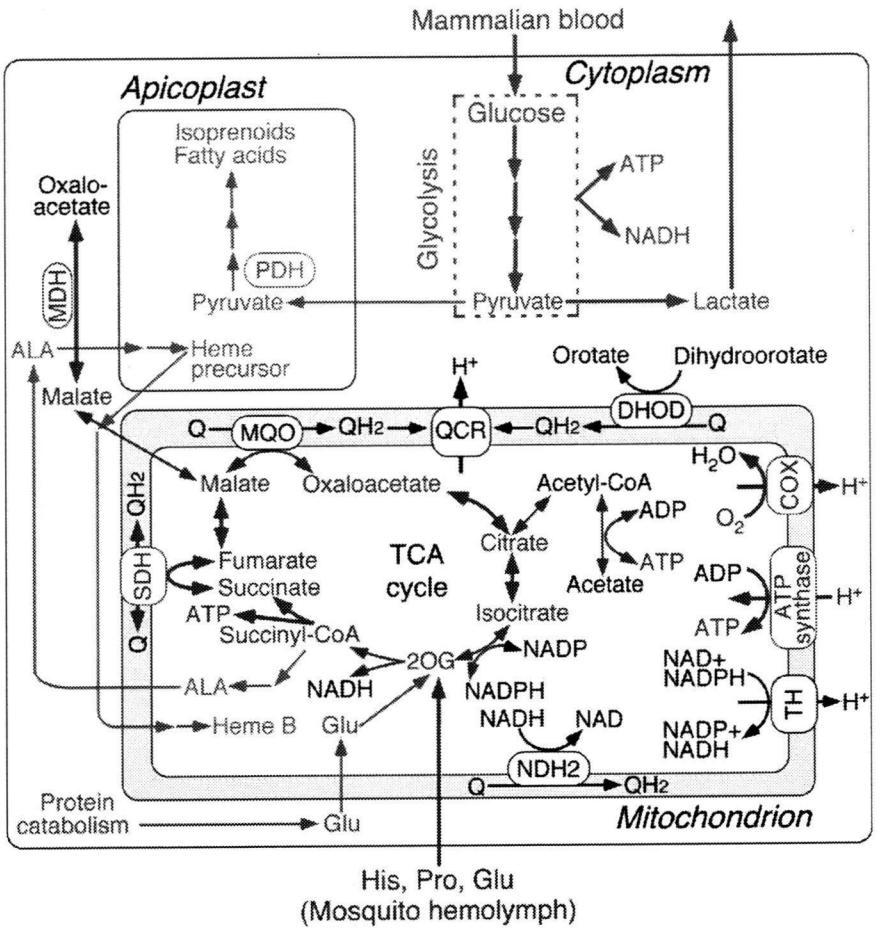

Fig. 1. Metabolic pathway in the human malaria parasite *P. falciparum*. Proton translocation machineries in the mitochondrion are F_oF_1-ATP synthase (ATPase), quinol–cytochrome *c* reductase (QCR), cytochrome *c* oxidase (COX), and NAD(P)-transhydrogenase (TH). Quinone reduction by alternative NADH dehydrogenase (NDH2), succinate dehydrogenase (SDH), malate:quinone oxidoreductase (MQO), and dihydroorotate dehydrogenase (DHOD) do not generate the proton-motive force. NAD-dependent malate dehydrogenase (MDH) and pyruvate dehydrogenase (PDH) are located in the cytoplasm and apicoplast, respectively, and do not participate in TCA cycle. Expression levels of MDH and TCA cycle enzymes (fumarate hydratase, SDH1, succinyl-CoA synthase α subunit, aconitase, and citrate synthase), and α and β subunits of ATP synthase are increased in salivary gland sporozoites while the expression levels of glycolysis pathway enzymes (hexokinase, phosphoglycerate kinase, pyruvate kinase and 6-phosphofructokinase) are increased in asexual blood-stage trophozoites and schizonts [Lasonder et al., 2008; Lasonder, Stunnenberg, personal communication]. A major carbon flow in blood-stage parasites is shown in *red* and possible carbon and energy flow in mosquito stages is shown in *blue*. Pathways absent in *B. bovis* are indicated by *green*. For the clarity, outer membranes of the mitochondrion and apicoplast are not shown. Abbreviations for metabolites are ALA (δ-aminolevulinic acid), DHAP (dihydroxyacetone phosphate), GA3P (glyceraldehyde-3-phosphate), and PEP (phosphoenolpyruvate).

the reductive and oxidative pathways. The resulting NADH and quinols are reoxidized by the respiratory chain, which indirectly drives ATP synthesis by the generation of proton-motive force.

In contrast to *P. falciparum*, the mitochondrion isolated from the erythrocytic stage rodent malaria parasite is cristate and contains more cytochromes (Fry and Beesley, 1991). Succinate respiration, ATP synthesis, and the collapse of the mitochondrial membrane potential by atovaquone (Srivastava et al., 1997), a potent inhibitor of ubiquinol–cytochrome *c* reductase (Complex III), suggest the presence of a functional oxidative phosphorylation system in the erythrocytic rodent parasite mitochondria (Uyemura et al., 2000, 2004). Transcriptome analysis of the erythrocytic human parasites, which have been isolated from infected patients, indicates that canonical mitochondrial functions exist to some extent in the human parasites (Daily et al., 2007). In *Plasmodium* spp., nuclear and mitochondrial genomes encode ubiquinol–cytochrome *c* reductase (QCR, Complex III), cytochrome *c* oxidase (COX, Complex IV), F_oF_1-ATP synthase (Complex V) and all the TCA cycle enzymes including succinate dehydrogenase (SDH, succinate–ubiquinone reductase, Complex II) (Carlton et al., 2002; Gardner et al., 2002). H^+-translocating NADH–ubiquinone reductase (NDH1, Complex I) in the mitochondrial respiratory chain is substituted by alternative NADH dehydrogenase (NDH2, a single-subunit NADH–ubiquinone reductase) (Uyemura et al., 2004; Biagini et al., 2006; Kawahara et al., 2009) (Fig. 1).

It should be noted that the membrane anchor subunits of Complex II (SDH3 (CybL) and SDH4 (CybS)) and of ATP synthase (subunits *a* (ATP6) and *b* (ATP4)) are not annotated in the current database (Carlton et al., 2002; Gardner et al., 2002), even though they are essential for transfer of chemical energy to ubiquinone and proton translocation, respectively (Fig. 2). Accordingly, the complete ATP synthase is assumed to be absent in *Plasmodium* spp. (Carlton et al., 2002; Gardner et al., 2002; Fry et al., 1990; Vaidya and Mather, 2005).

Recently, we characterized characterized Complex II of the erythrocytic stage *Plasmodium yoelii yoelii* mitochondria and found evidence for the presence of SDH3 and SDH4 (Kawahara et al., 2009). Because of the low expression of TCA cycle enzymes in

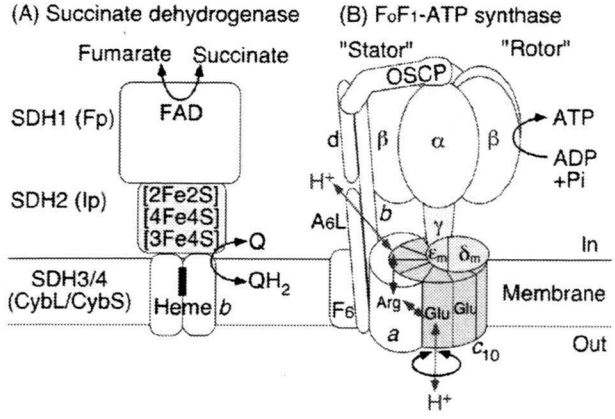

Fig. 2. Structure model for protist Complex II and ATP synthase.

the erythrocytic stage cells (Lasonder et al., 2008), sequence analysis of the anchor subunits was difficult in the *Plasmodium* mitochondria. Here we report candidates for the membrane anchor subunits of the *Plasmodium* oxidative phosphorylation enzymes. SDH3 and SDH4 of Complex II were identified by using structural fingerprints as probes while subunits *a* and *b* of ATP synthase were identified by BLAST search with proteomics data from other protists. Assignment of the membrane anchors of *Plasmodium* Complex II and ATP synthase will help our understanding of energy metabolism and the development of new antimalarials.

2. Materials and methods

2.1. Analytical methods

The presence of structural fingerprints (i.e., the heme/quinone-binding motifs) in ORFs shared by *P. falciparum* and *P. y. yoelii* genomes in the TIGR Parasite Database (http://www.tigr.org/tdb/e2k1/pya1/pya1-ortho.shtml/) was examined manually. Database searches using protein sequences were performed with the BLAST service at NCBI (http://www.ncbi.nlm.nih.gov/), GeneDB (http://www.genedb.org/), PlasmoDB (http://plasmodb.org/plasmo/), and TBestDB (http://tbestdb.bcm.umontreal.ca/). Sequences were aligned with ClustalX 2.0 (Larkin et al., 2007) and manual adjustments were made if needed. Transmembrane regions were identified with TMHMM (http://www.cbs.dtu.dk/services/TMHMM/).

3. Results and discussion

3.1. Evidence for the presence of membrane anchors of Plasmodium Complex II

Mammalian Complex II belongs to type C Complex II (Hägerhäll, 1997) and consists of four subunits and is bound to the matrix side of the inner mitochondrial membrane (Cecchini, 2003). A flavoprotein subunit (Fp, SDH1) and an iron–sulfur subunit (Ip, SDH2) form a soluble heterodimer, which then binds to a membrane anchor *b*-type cytochrome (SDH3/SDH4 heterodimer). SDH1 contains a covalently bound FAD and transfers electrons from succinate to the iron–sulfur clusters in SDH2. Electrons are then transferred to ubiquinone within a binding pocket provided by SDH2 and the SDH3/SDH4 heterodimer (Yankovskaya et al., 2003; Sun et al., 2005; Yang et al., 1998; Horsefield et al., 2006). Bacterial and mitochondrial SDH3 and SDH4 generally consist of three transmembrane helices (TM) each (I–III and IV–VI, respectively) (Yankovskaya et al., 2003; Sun et al., 2005). The quinone/heme-binding motifs, "RPx$_{16}$Sx$_2$HR" in TM-I and "Hx$_{10}$D" in TM-II of SDH3 and "Hx$_{10}$DY" in TM-V of SDH4 can be identified by sequence comparisons (Figs. 3 and 4). Arg31 (*Escherichia coli* Complex II numbering) in the SDH3 Sx$_2$HR motif and Asp82 in the SDH4 Hx$_{10}$DY motif are in close proximity to ubiquinone and could interact with Tyr83 (Yankovskaya et al., 2003). Ser27 in the SDH3 Sx$_2$HR motif has been shown to be essential for quinone binding (Yang et al., 1998) and is a candidate for hydrogen bonding to the O$_4$ atom of ubiquinone (Horsefield et al., 2006). Tyr83 in the SDH4 Hx$_{10}$DY motif could hydrogen bond to the O$_1$ atom of ubiquinone and contribute to the binding affinity (Yankovskaya et al., 2003; Horsefield et al., 2006). Examination of the *E. coli* Complex II structure (PDB 1NEK) suggests that the first arginine (Arg9 in *E. coli* SDH3) in the RPx$_{16}$Sx$_3$R motif is in the vicinity of Glu186 in SDH1 and Asp106 in SDH2 and may play a structural role through a hydrogen bond network. Histidines in helices II and V (His84 and His 71 in *E. coli* SDH3 and SDH4, respectively) serve as the axial ligands for heme *b* (Yankovskaya et al., 2003; Sun et al., 2005) (Fig. 4A) but are dispensable for assembly and quinone reduction (Tran et al., 2007; Oyedotun et al., 2007).

Earlier, we have cloned and sequenced genes coding for the *P. falciparum* SDH1 and SDH2 by homology probing (Takeo et al., 2000). In contrast to these subunits, *Plasmodium* SDH3 and SDH4 appear to be highly divergent from their mitochondrial orthologs and are not annotated in the current database at NCBI, GeneDB and PlasmoDB. The *P. falciparum* Complex II previously isolated from whole cell lysates was found to be the SDH1/SDH2 heterodimer with an apparent molecular weight of 90 kDa (Suraveratum et al., 2000). The authors claimed that *Plasmodium* Complex II has a much lower K_m (3 μM) for succinate than mammalian enzymes and has the plumbagin-sensitive succinate–quinone reductase activity. However, the concentration (0.2%) of the non-ionic detergent octyl glucoside used for the isolation of *P. falciparum* Complex II was insufficient to solubilize all membrane proteins (i.e., the critical micelle concentration of octyl glucoside is 0.73%). Octyl glucoside likely dissociates the SDH1/SDH2 dimer from the membrane anchors and the aerobic isolation of the SDH1/SDH2 dimer would likely damage the iron–sulfur clusters in SDH2. Thus, the enzyme activities of such preparations need to be carefully examined. Recently, we identified *P. y. yoelii* Complex II as a 135-kDa band by native PAGE followed by activity staining (Kawahara et al., 2009). 2D-PAGE analysis of the Complex II revealed the presence of two small subunits, candidates for *Plasmodium* SDH3 and SDH4. The succinate–quinone reductase activity of *P. falciparum* and *P. y. yoelii* mitochondria (Takashima et al., 2001; Mi-Ichi et al., 2005; Kawahara et al., 2009) and succinate respiration in rodent malaria mitochondria (Uyemura et al., 2000, 2004) support the presence of membrane anchor subunits of Complex II for transferring electron to ubiquinone molecule within the inner mitochondrial membrane.

3.2. Identification of Plasmodium Complex II anchor subunits

Protist SDH3 and SDH4 are generally divergent from their orthologs, so conventional BLAST programs using bacterial and eukaryotic sequences as queries failed to identify *Plasmodium* subunits in the current genome database. Recently, we purified Complex II from the parasitic protist *Trypanosoma cruzi* and identified six each of hydrophilic and hydrophobic subunits by protein sequencing (Morales et al., 2009). Supernumerary non-catalytic

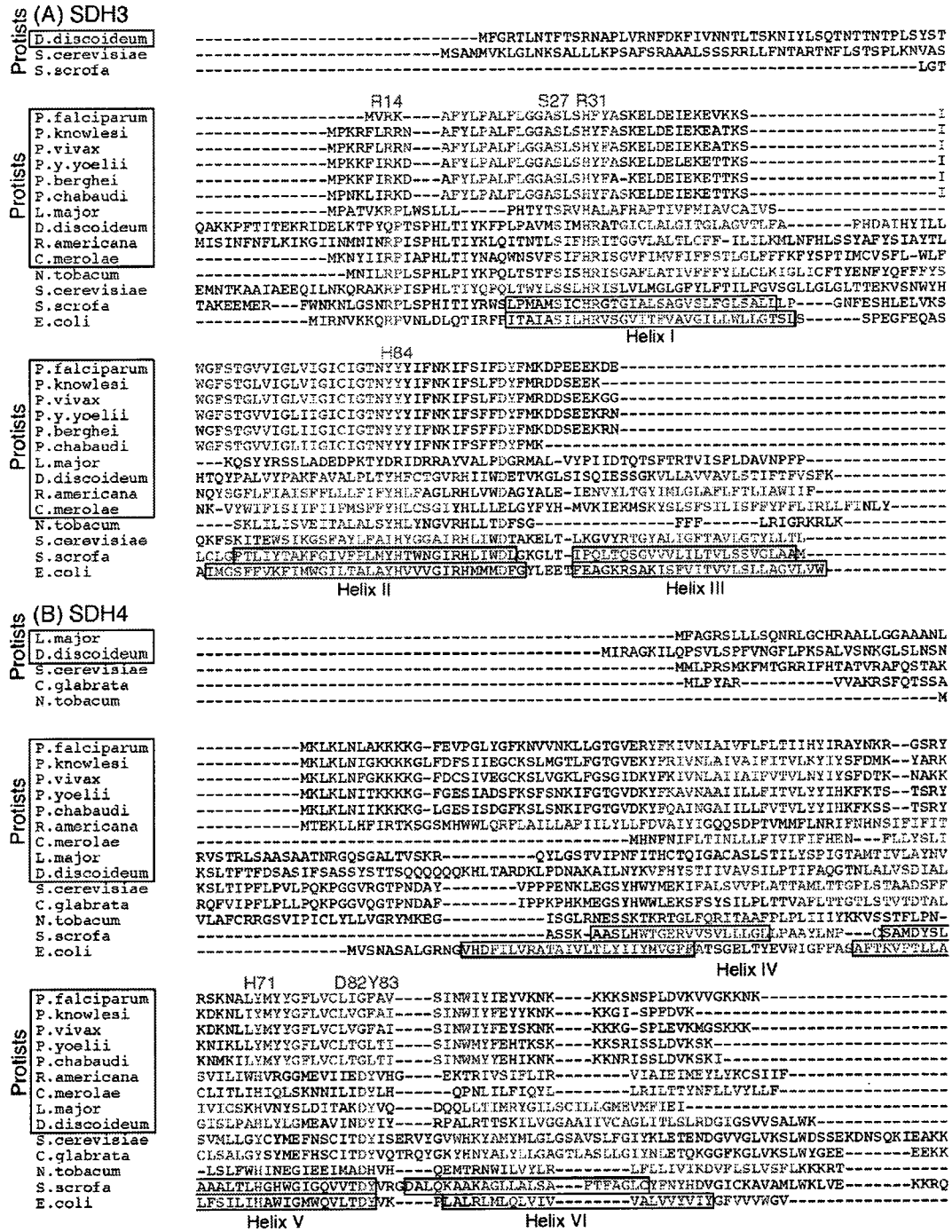

Fig. 3. Sequence alignment of SDH3 (A) and SDH4 (B) of *Plasmodium* Complex II. SDH3 and SDH4 sequences (GenBank accession Nos.) used are *P. falciparum* (XP_966100, XP_001347385), *P. knowlesi* (PKH_113810, PKH_080980), *P. vivax* (XP_001616129, XP_001614414), *P. y. yoelii* (XP_731082, XP_726783), *P. berghei* (XP_678526, not available), *P. chabaudi* (XP_742786, XP_738723), *Leishmania major* (XP_848167, XP_001685874), *Dictyostelium discoideum* (XP_643757, XP_642171), *Reclinomonas americana* (NP_044796, NP_044797), *Cyanidioschyzon merolae* (NP_059349, NP_059380), *Nicotiana tabacum* (YP_173376, YP_173457), *S. cerevisiae* S288C (NP_012781, NP_010463), *Candida glabrata* (not used, XP_446226), *Sus scrofa* (1ZOY_C, 1ZOY_D), and *E. coli* (NP_415249, NP_415250). Amino acid residues proposed for binding of ubiquinone and protoheme IX are shown in *red* and transmembrane regions predicted by TMHMM are in *blue*. Residue numbers refer to the *E. coli* SDH3 (SdhC) and SDH4 (SdhD) sequences. Transmembrane helices found in porcine Complex II (PDB 1ZOY) and *E. coli* Complex II (PDB 1NEK) are boxed.

subunits in *T. cruzi* Complex II may have evolved by complementary degeneration of dispersed duplicates (Hurles, 2004) in the Euglenozoa. Among six transmembrane subunits, we identified *T. cruzi* SDH3 and SDH4 on the basis of the presence of the quinone/heme-binding motifs, that are only conserved in these candidates (Morales et al., 2009).

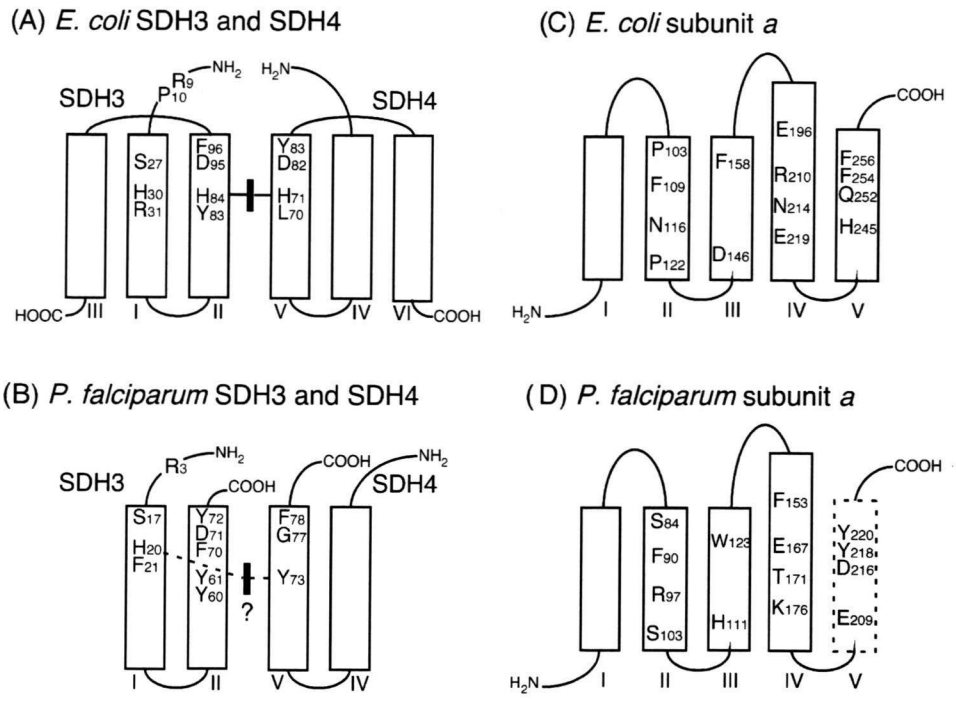

Fig. 4. Proposed structures for SDH3 and SDH4 of Complex II and subunits *a* from *E. coli* and *P. falciparum*.

Unlike *T. cruzi* mitochondria, the yield of *Plasmodium* mitochondria and the specific activity of Complex II were very low (Takashima et al., 2001; Mi-Ichi et al., 2005; Kawahara et al., 2009). Therefore, we took an alternative strategy for the identification of *Plasmodium* SDH3 and SDH4. We reexamined manually the sequences of *Plasmodium* membrane proteins for the presence of the quinone/heme-binding motifs of SDH3 and SDH4. Among 3310 ORFs[1] conserved in both *P. falciparum* and *P. y. yoelii* at the TIGR Parasite Database, 15.5% are membrane proteins with putative transmembrane segments, and 2.5% are shorter than 200 amino acid residues, as are the mitochondrial SDH3 and SDH4. From screening based on the number of TMs (1–3), spacing between TMs, conservation in *Plasmodium* spp., and the sequence motifs in transmembrane helices, we identified candidates for *P. falciparum* SDH3 (83 residues, GenBank accession No. XP_966100) and SDH4 (118 residues, XP_001347385) with two putative transmembrane helices (Figs. 3 and 4B, Table 1), which lack helices III and VI, respectively. Sequence identities of *P. falciparum* SDH3 and SDH4 against counterparts in *E. coli* and *Homo sapiens* are 15.7% and 14.3%, respectively, and 23.1% and 21.7%, respectively. An alternative candidate for PfSDH4 (XP_001349911 with one TM) contains the "YHx$_9$DY" motif but TMHMM predicts that this motif is in the C-terminal hydrophilic tail. Orthologs of PfSDH3 and PfSDH4 are present in human malaria parasites *Plasmodium vivax* and *Plasmodium knowlesi* and rodent malaria parasites *P. y. yoelii*, *Plasmodium berghei* and *Plasmodium chabaudi* in the current database[2]. Phylogenetic analysis of amino acid sequences showed that a clade for the membrane anchors of *Plasmodium* and Euglenozoa Complex II is an outgroup of bacterial and mitochondrial SDH3 and SDH4 (Fig. 5).

Table 1
Oxidative phosphorylation systems in *P. falciparum*.

Enzyme	Subunits	GenBank accession no.
NDH_2		XP_001352022
Succinate–quinone reductase	SDH1	XP_001347618
	SDH2	XP_001350535
	SDH3	XP_966100
	SDH4	XP_001347385
Ubiquinol:cytochrome *c* oxidoreductase	Cyt *b*	NP_059668[a]
	Rieske FeS	XP_001348547
	Cyt c_1	XP_001348771
	Hinge (QCR6)	XP_001348422
	MPP	XP_001351788, XP_001352201
Cytochrome *c*	Cyc1	XP_001348211
Cytochrome *c* oxidase	COX I	NP_059667[a] XP_001350328
	COX II	$(2_N)^b$, XP_001348462 $(2_C)^b$
	COX III	NP_059666[a]
	COX V	XP_001352148
	COX VI	XP_001352150
	COX VII	CAX64384
	COX VIII	XP_001351632
ATP synthase	ATP1 (α)	XP_001349675
	ATP2 (β)	XP_001350751
	ATP3 (γ)	XP_001349841
	ATP5 (OSCP, δ)	XP_001349828
	ATP16 (δ_m, ε)	XP_001348152
	ATP15 (ε_m)	XP_001349058
	ATP7 (d, p18)	XP_001348820
	ATP6 (*a*)	XP_001347344
	ATP4 (*b*)	XP_001348969
	ATP9 (*c*)	MAL7P1.340
Dihydroorotate dehydrogenase		XP_966023
NAD(P)-transhydrogenase		XP_001348682

[a] Heterodimeric COX II consist of two degenerated subunits, which retains the *N*- or *C*-terminal functional domain.

[1] Re-examination of the annotation of the *P. y. yoelii* genome on the basis of a detailed analysis of a comprehensive set of cDNA sequences and the liver stage proteome identified a further 510 genes which have orthologs in the *P. falciparum* genome (Vaughan et al., 2008). Analysis of these sequences did not yield any candidates for Complex II SDH3 and SDH4 and ATP synthase subunits *a* and *b*.

[2] The PbSDH3 sequence seems incomplete and the PbSDH4 sequence has not been identified yet at GeneDB. At NCBI, PfSDH3 was identified in *Toxoplasma gondii* and the alternative PfSDH4 was found in other *Plasmodium* species, *T. gondii*, *Babesia bovis*, and *Theileria parva*.

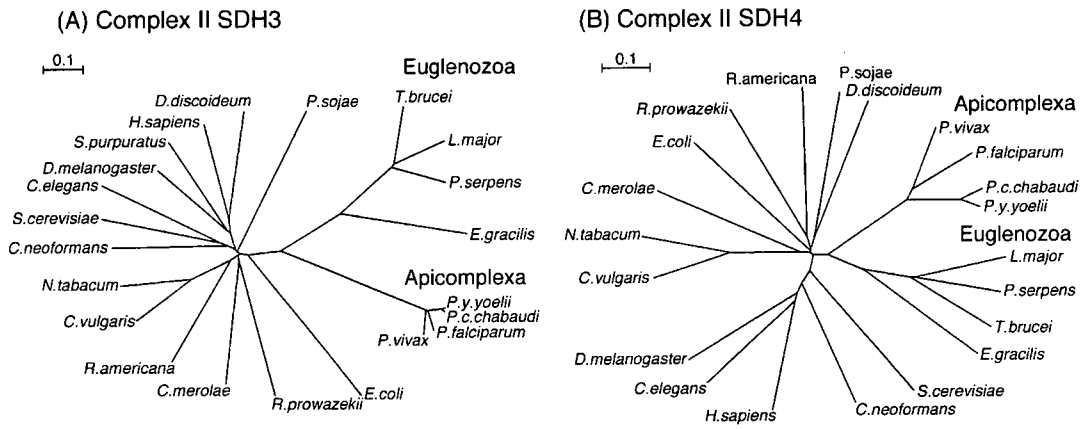

Fig. 5. Unrooted phylogenetic trees for SDH3 and SDH4 of Complex II. SDH3 and SDH4 sequences (GenBank accession Nos.) used are *H. sapiens* (NP_002992, NP_002993), *Caenorhabditis elegans* (NP_499283, NP_496369), *Cryptococcus neoformans* (XP_566692, XP_569088), *T. brucei* (XP_845531, XP_823384), *Phytomonas serpens* (CO723838, CO723900), *Euglena gracilis* (EC671331, EC610072), and *Rickettsia prowazekii* (NP_220518, NP_220519). All other sequences are described in the legend to Fig. 3.

3.3. Heme and quinone binding sites of Plasmodium Complex II

In *Plasmodium*, SDH3 contains an "$Rx_{13-14}Sx_2HY(F)$" motif in the *N*-terminal region of helix I and a "$YYx_{10}DY$" motif in the *C*-terminal region of helix II, in place of "$RPx_{16}Sx_2HR$" and "$YHx_{10}D$" motifs in other organisms (Figs. 3 and 4). *Plasmodium* SDH4 contains a "$Yx_{10}G$" motif in helix V in place of the canonical "$Hx_{10}DY$" motif (Figs. 3 and 4). Sequence alignments indicate that the tyrosines may substitute

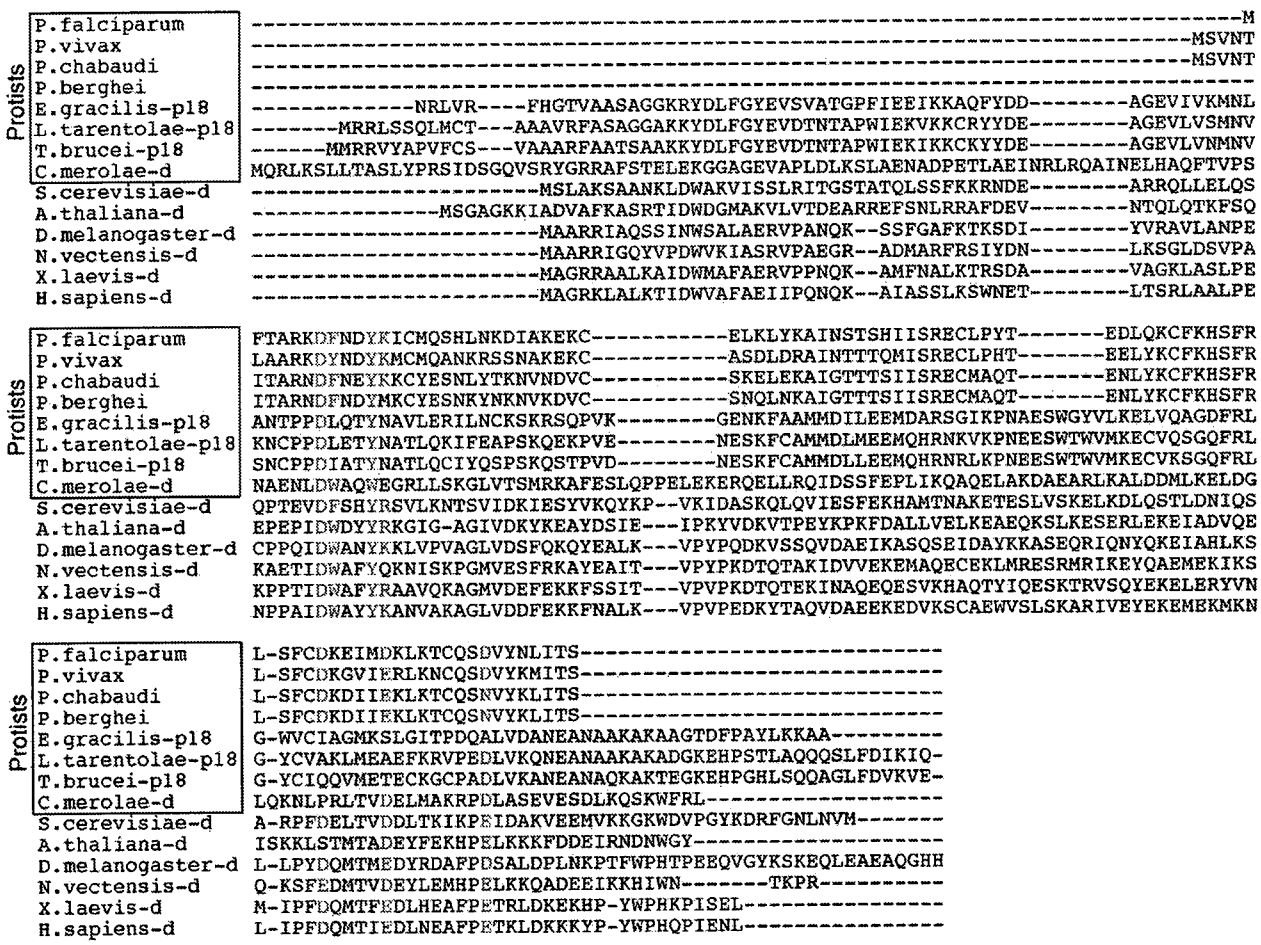

Fig. 6. Sequence alignment of subunit *d* (ATP7) of protist ATP synthase. Sequences used (GenBank accession No.) are *P. falciparum* (XP_001348820), *P. vivax* (PVX_117075), *P. c. chabaudi* (PCAS_133570), *P. berghei* (PB001416.02.0), *E. gracilis* (EC671747), *Leishmania tarentolae* (Q25423; p18), *T. brucei* (XP_844845; p18), *S. cerevisiae* (NP_012909), *Arabidopsis thaliana* (NP_190798), *Drosophila melanogaster* (NP_524402), *Nematostella vectensis* (XP_001626831), *Xenopus laevis* (NP_001084746), and *H. sapiens* (NP_006347). *C. merolae* subunit *d* sequence (CMK178C) was obtained at *Cyanidioschyzon merolae* Genome Project.